Biogeosciences Discuss., 12, 13427–13481, 2015
www.biogeosciences-discuss.net/12/13427/2015/
doi:10.5194/bgd-12-13427-2015

Biogeosciences
Discussions
Open Access

Mediterranean climate since the Middle Pleistocene: a 640 ka stable isotope record from Lake Ohrid (Albania/Macedonia)

J. H. Lacey[1,2], M. J. Leng[1,2], A. Francke[3], H. J. Sloane[2], A. Milodowski[4], H. Vogel[5], H. Baumgarten[6], and B. Wagner[3]

[1]Centre for Environmental Geochemistry, School of Geography, University of Nottingham, Nottingham, NG7 2RD, UK
[2]NERC Isotope Geosciences Facilities, British Geological Survey, Keyworth, Nottingham, NG12 5GG, UK
[3]Institute of Geology and Mineralogy, University of Cologne, 50674 Cologne, Germany
[4]British Geological Survey, Keyworth, Nottingham, NG12 5GG, UK
[5]Institute of Geological Sciences and Oeschger Centre for Climate Change Research, University of Bern, 3012 Bern, Switzerland
[6]Leibniz Institute for Applied Geophysics, 30655 Hanover, Germany

Received: 28 July 2015 – Accepted: 4 August 2015 – Published: 20 August 2015

Correspondence to: J. H. Lacey (jack.lacey@nottingham.ac.uk)

Published by Copernicus Publications on behalf of the European Geosciences Union.

Abstract

Lake Ohrid (Macedonia/Albania) is an ancient lake with a unique biodiversity and a site of global significance for investigating the influence of climate, geological and tectonic events on the generation of endemic populations. Here, we present oxygen ($\delta^{18}O$) and carbon ($\delta^{13}C$) isotope data on carbonate from the upper ca. 248 m of sediment cores recovered as part of the Scientific Collaboration on Past Speciation Conditions in Lake Ohrid (SCOPSCO) project, covering the past 640 ka. Previous studies on short cores from the lake (up to 15 m, < 140 ka) have indicated the Total Inorganic Carbon (TIC) content of sediments to be highly sensitive to climate change over the last glacial–interglacial cycle, comprising abundant endogenic calcite through interglacials and being almost absent in glacials, apart from discrete bands of early diagenetic authigenic siderite. Isotope measurements on endogenic calcite ($\delta^{18}O_c$ and $\delta^{13}C_c$) reveal variations both between and within interglacials that suggest the lake has been subject to hydroclimate fluctuations on orbital and millennial timescales. We also measured isotopes on authigenic siderite ($\delta^{18}O_s$ and $\delta^{13}C_s$) and, with the $\delta^{18}O_c$ and $\delta^{18}O_s$, reconstruct $\delta^{18}O$ of lakewater ($\delta^{18}O_{lw}$) through the 640 ka. Overall, glacials have lower $\delta^{18}O_{lw}$ when compared to interglacials, most likely due to cooler summer temperatures, a higher proportion of winter precipitation (snowfall), and a reduced inflow from adjacent Lake Prespa. The isotope stratigraphy suggests Lake Ohrid experienced a period of general stability through Marine Isotope Stage (MIS) 15 to MIS 13, highlighting MIS 14 as a particularly warm glacial, and was isotopically freshest during MIS 9. After MIS 9, the variability between glacial and interglacial $\delta^{18}O_{lw}$ is enhanced and the lake became increasingly evaporated through to present day with MIS 5 having the highest average $\delta^{18}O_{lw}$. Our results provide new evidence for long-term climate change in the northern Mediterranean region, which will form the basis to better understand the influence of major environmental events on biological evolution within the lake.

BGD

12, 13427–13481, 2015

1 Introduction

Global climate models indicate the Mediterranean to be a highly vulnerable area with respect to predicted future changes in temperature and precipitation regimes (Giorgi, 2006; Giannakopoulos et al., 2009), and the associated stress on water resources may have important socio-economic impacts across the region (García-Ruiz et al., 2011). It is therefore vital to investigate the regional response to past climate fluctuations and improve our understanding of global climate dynamics as a prerequisite for establishing future scenarios (Leng et al., 2010a). Stable isotope ratios preserved in sedimentary lacustrine carbonates are a proxy for past climate and hydrological change (Leng and Marshall, 2004), and combinations of lake records can be used to assess the spatial coherence of isotope variations (Roberts et al., 2008). Although there are numerous stable isotope records from the Mediterranean, for example from marine sediment cores (Piva et al., 2008; Maiorano et al., 2013) and speleothems (Bar-Matthews et al., 2003; Antonioli et al., 2004), those from lacustrine carbonate are typically confined to the Holocene age (Dean et al., 2013; Francke et al., 2013) and only a limited number of records extend beyond the Last Glacial (Frogley, 1999; Kwiecien et al., 2014).

Lake Ohrid, located on the Balkan Peninsula in south-eastern Europe, is thought to be among the oldest extant lakes on Earth with a limnological age in excess of 1.2 million years (Wagner et al., 2014; Lindhorst et al., 2015). So called ancient lakes are often associated with an outstanding degree of natural biodiversity, and Ohrid is one of only several lakes worldwide to contain such a varied assemblage with over 210 described endemic species (Albrecht and Wilke, 2008). Within the research framework of the Scientific Collaboration on Past Speciation Conditions in Lake Ohrid (SCOPSCO) project, extended and more precise past climate information are needed to support assessment of the influence of climate shifts on the evolution of taxa within the lake and to infer teleconnections between other long and continuous records.

Previous core sequences from Lake Ohrid span the past 140 000 years and indicate the lake to be highly sensitive to millennial-scale variations in global climate (e.g. Vogel

BGD
12, 13427–13481, 2015

et al., 2010; Wagner et al., 2010). Several of these cores have been analysed for the isotope composition of carbonate over the last glacial–interglacial cycle, including on fine grained calcite (endogenic) from bulk sediment (Leng et al., 2010a; Lacey et al., 2014) and benthic ostracods (Belmecheri et al., 2010), however the current isotope datasets do not have the temporal extent necessary to meet the primary research aims of the SCOPSCO project (Wagner et al., 2014). Here, we present new stable isotope data on carbonate (both endogenic calcite and authigenic siderite) from SCOPSCO cores, covering approximately ca. 640 ka (Baumgarten et al., 2015; Francke et al., 2015), and reconstruct the oxygen isotope composition of lakewater ($\delta^{18}O_{lw}$) using the calcite and siderite isotope data. This will provide valuable information on the magnitude and timing of Late Quaternary climate oscillations and enable us to compare the structure and consistency of interglacial and glacial periods through the last 15 Marine Isotope Stage (MIS).

2 General setting

Lake Ohrid (Former Yugoslav Republic of Macedonia/Republic of Albania) is situated at 693 m a.s.l. and formed in a tectonic graben bounded by high mountain chains to the west and east (Fig. 1). The lake has a maximum length of 30.8 km, a maximum width of 14.8 km, an area of 358 km^2 and a volume of 50.7 km^3 (Stankovic, 1960; Popovska and Bonacci, 2007); the basin has a simple bath tub-shaped morphology with a maximum and average water depth of 293 and 150 m respectively (Lindhorst et al., 2015). There is a relatively small catchment area of 2600 km^2, even accounting for input from neighbouring Lake Prespa, which delivers water through a network of karst aquifers thought to correspond to 53 % of total water input (Matzinger et al., 2006a). The subterranean connection has been confirmed using tracer experiments (Anovski et al., 1991; Amataj et al., 2007) and feeds spring complexes mainly to the south-east of the lake (Eftimi and Zoto, 1997; Matzinger et al., 2006a). The remaining input comprises river inflow and direct precipitation on the lake's surface. Water output is via the River Crn Drim on the northern margin (66 %) and by means of evaporation (34 %) (Matzinger et al., 2006b). Lake Ohrid has a long hydraulic residence time (ca. 80 years) and complete overturn is thought to occur approximately every 7 years (Hadzisce, 1966), which leads to de-stratification of the water column during deep convective winter mixing (Matzinger et al., 2006b).

Mediterranean climate is generally influenced by the sub-tropical anticyclone in summer and mid-latitude westerlies during winter, providing a complex and sensitive climatology at a major transition zone between temperate and arid domains (Magny et al., 2013). This leads to a precipitation seasonality controlled by the southward migration of the Intertropical Convergence Zone during winter, allowing the influence of westerlies to be established, and the development of cyclogenesis across the whole Mediterranean (Tzedakis et al., 2009a). Local orography produces climatic sub-zones with variable distributions of precipitation and temperature across the Mediterranean (Zanchetta et al., 2007), and the climate of Lake Ohrid and its watershed is controlled by both sub-Mediterranean and continental influences owing to its location in a deep basin sheltered by mountains and its proximity to the Adriatic Sea (Vogel et al., 2010; Panagiotopoulos et al., 2013). Today, air temperatures range between a minimum of −6 °C and a maximum of +32 °C, and have an annual average of around +10 °C (Fig. 2; Popovska and Bonacci, 2007). Lake Ohrid surface water temperature remains between +6 and +26 °C and bottom water temperature is constant between +5 and +6 °C (Popovska and Bonacci, 2007). The catchment receives an average annual rainfall of around 900 mm and the prevailing winds trace the Ohrid valley (Stankovic, 1960).

3 Material and methods

3.1 Core recovery

The ICDP SCOPSCO coring campaign of spring 2013 was a resounding success with over 2100 m of sediment recovered from different 4 sites; a full overview of coring loca-

BGD
12, 13427–13481, 2015

tions, processes and initial data are given by Wagner et al. (2014). To summarise, drill sites were selected based on hydro-acoustic and seismic surveys carried out between 2004 and 2008, which show the main target location to be in the thick undisturbed sediments of the central basin with an estimated continuous sedimentary fill of up to 680 m. Coring at the "DEEP" site (5045-1; 41°02′57″ N, 020°42′54″ E) used the Deep Lake Drilling System operated by DOSECC to reach a maximum sediment depth of 569 m below lake floor (m b.l.f.) and returned a 95 % complete composite profile containing 1526 m of core in total (99 % recovery for the upper 430 m). The cores were subsequently correlated, processed, opened and sampled at the University of Cologne (as described by Francke et al., 2015). Total inorganic carbon (TIC) data was measured by Francke et al. (2015) using a DIMATOC 100 carbon analyser (Dimatec Corp., Germany).

3.2 Analytical work

The DEEP site composite profile was sampled for oxygen and carbon isotope ratios on carbonate at 16 cm intervals from the surface to a correlated depth of 247.79 m, throughout zones with a high carbonate content (up to 10 % TIC thought to represent interglacials). The carbonate within these zones predominantly comprises calcite. Idiomorphic calcite crystals and crystal clusters between 20–100 µm have been reported from previous Scanning Electron Microscopy (SEM) investigations, which show the crystals to be dominantly $CaCO_3$ (Wagner et al., 2008; Matter et al., 2010). The size and shape of the crystals are typical of endogenic precipitation (Leng et al., 2010b; Lézine et al., 2010), and although $CaCO_3$ crystals recovered from sediment traps are generally pristine (Matter et al., 2010), those from core material are typically characterised by partial dissolution (Wagner et al., 2009).

Within zones of overall low TIC, intermittent spikes to higher TIC were also sampled and the constituent carbonate species investigated using X-Ray Diffraction (XRD), as X-Ray Fluorescence (XRF) showed the recurrent spikes were high in Fe and Mn (Francke et al., 2015). XRD was conducted on a PANalytical X'Pert Pro powder diffrac-

BGD
12, 13427–13481, 2015
Mediterranean climate since the Middle Pleistocene
J. H. Lacey et al.

tometer, with Cobalt K_{α_1} radiation over the scan range 4.5–85° 2θ and a step size of 2.06° $2\theta\,min^{-1}$. Phase identification was conducted using PANalytical HighScore Plus version 4.0 analytical software interfaced with the latest version of the International Centre for Diffraction Data (ICDD) database. The XRD analysis showed the carbonate in the samples to be composed of siderite, which was confirmed using Energy-Dispersive X-Ray Spectroscopy (EDX) on epoxy resin-embedded thin sections.

Relative concentration changes of the carbonate phases (calcite and siderite) were determined at 32 cm intervals from the surface to a correlated depth of 247.79 m using Fourier transform infrared spectroscopy (FTIRS). For FTIRS analysis, 0.011 ± 0.0001 g of each sample was mixed with 0.5 ± 0.0001 g of oven-dried spectroscopic grade potassium bromide (KBr) (Uvasol®, Merck Corp.) and subsequently homogenized using a mortar and pestle. A Bruker Vertex 70 equipped with a MCT (Mercury–Cadmium–Telluride) detector, a KBr beam splitter, and a HTS-XT accessory unit (multi-sampler) was used for the measurement. Each sample was scanned 64 times at a resolution of $4\,cm^{-1}$ (reciprocal centimetres) for the wavenumber range from 3750 to $520\,cm^{-1}$ in diffuse reflectance mode. FTIRS analysis was performed at the Institute of Geological Sciences, University of Bern, Switzerland. Linear baseline correction was applied to normalize the recorded FTIR spectra and to remove baseline shifts and tilts by setting two points of the recorded spectrum to zero (3750 and 2210–$2200\,cm^{-1}$). Peak areas diagnostic for bending vibrations of the carbonate ion in calcite (707–$719\,cm^{-1}$) and siderite (854–$867\,cm^{-1}$) and representative for their relative abundance (White, 1974; Chukanov, 2014) were integrated using the OPUS (Bruker Corp.) software package.

For the isotope analysis approximately 250 mg (calcite) or 1000 mg (siderite) of sample was disaggregated in 5 % sodium hypochlorite solution for 24 h to oxidise reactive organic material, then washed in deionised water to neutral pH, dried at 40 °C and ground. To evolve CO_2 for isotope analysis, calcite-bearing samples were reacted overnight inside a vacuum with anhydrous phosphoric acid at a constant 25 °C, and siderite-bearing samples were reacted with anhydrous phosphoric acid within a vacuum for 96 h at 100 °C. For both types of sample CO_2 was cryogenically separated

BGD
12, 13427–13481, 2015

from water vapour under vacuum and analysed using a VG Optima dual inlet mass spectrometer. The mineral-gas fractionation factor used for calcite was 1.01025 and for siderite was 1.00881 (derived from Rosenbaum and Sheppard, 1986). The oxygen and carbon isotope composition of calcite ($\delta^{18}O_c$ and $\delta^{13}C_c$) and siderite ($\delta^{18}O_s$ and $\delta^{13}C_s$) are reported as per mille (‰) deviations of the isotope ratios ($^{18}O/^{16}O$ and $^{13}C/^{12}C$) calculated to the V-PDB scale. Within-run laboratory standards were utilised for which analytical reproducibility was < 0.1 ‰ for $\delta^{18}O$ and $\delta^{13}C$.

4 Chronology

The age model for the upper 247.79 m of the DEEP site sequence was established by (1) using tephrostratigraphical information (1st order tie points), (2) tuning TOC (and TOC related proxies) to trends in local daily insolation patterns (26 June at 41° N; Laskar et al., 2004) and the winter season length (2nd order tie points), and (3) tuning high TIC content to minima of the Lisiecki and Raymo (2005) global benthic isotope stack (LR04; 3rd order tie points) (Francke et al., 2015). The tie points comprised 9 tephra layers, correlated to well-known Italian volcanic eruptions by geochemical fingerprint analysis (age and error is based on recalibration of Ar/Ar ages from the literature by Leicher et al., 2015), and 45 cross correlation points. For each correlation point an error of ±1000 years was included in the age-depth calculation to account for inaccuracies in the tuning process (Francke et al., 2015). Finally, the age model for the sediment cores was cross-evaluated and fine tuned to the age model of the borehole logging data (Baumgarten et al., 2015). The latter is based on tuning *K* contents from downhole spectral gamma ray to LR04 and cyclostratigraphic analysis on gamma ray data. Chronological information and tie points are presented and discussed in detail in Francke et al. (2015), Leicher et al. (2015) and Baumgarten et al. (2015). The age model implies that the upper 247.79 m of the DEEP site composite profile represents the last ca. 640 ka and covers Marine Isotope Stages (MIS) 16–1 (Lisiecki and Raymo,

BGD
12, 13427–13481, 2015

2005), hereafter results are discussed within the MIS framework (lettered sub-stages after Railsback et al., 2015).

5 Results

Isotope data from core 5045-1 are shown in Fig. 3 with the high-resolution Holocene calibration data from the Lini site core Co1262 (Fig. 1; Lacey et al., 2014). Over the whole record, calcite occurs predominantly in interglacial and interstadial periods (i.e. odd-numbered MIS) and has mean $\delta^{18}O_c = -5.3 \pm 0.8$ ‰ (1σ, $n = 924$) and $\delta^{13}C_c$ + 0.4±0.6 ‰ (1σ, $n = 924$). MIS 15 and 13 have similar $\delta^{18}O_c$, TIC remains relatively high through glacial MIS 14 and $\delta^{18}O_c$ is consistent with the bounding MIS values (MIS 15 to MIS 13 mean $= -5.5 \pm 0.7$ ‰, 1σ, $n = 294$). Minimum $\delta^{18}O_c$ for the whole record (–7.6 ‰) occurs at ca. 378 ka during MIS 11, which has mean $\delta^{18}O_c = -5.5 \pm 0.9$ ‰ (1σ, $n = 75$) and the largest overall variation. MIS 9 has the lowest interglacial mean $\delta^{18}O_c$ of the record (-5.8 ± 0.9 ‰, 1σ, $n = 69$). A TIC spike centred around ca. 287 ka in MIS 8 has lower $\delta^{18}O_c$ than MIS 9 values (-6.5 ± 0.5 ‰, 1σ, $n = 18$). MIS 7 shows similar values to the lower core and has mean $\delta^{18}O_c = -5.5 \pm 0.6$ ‰ (1σ, $n = 73$). MIS 5 contains the highest mean $\delta^{18}O_c$ (-4.6 ± 0.8 ‰, 1σ, $n = 104$). Holocene $\delta^{18}O_c$ is similar to MIS 5 (-4.9 ± 0.7 ‰, 1σ, $n = 273$; Lacey et al., 2014).

The glacial period (even-numbered MIS) siderites occur in bands and their isotope composition is thought to reflect lakewater conditions at the time of precipitation, even though they may represent discrete events. The horizons were identified visually in the cores as lighter-coloured bands, and their composition was confirmed to be siderite using XRF (Francke et al., 2015), XRD and SEM-EDX. FTIRS indicates siderite to present predominantly in areas where TIC is negligible (glacial and stadial periods), with an increasing abundance up core (Fig. 3). Overall, mean $\delta^{18}O_s = -2.2 \pm 0.8$ ‰ (1σ, $n = 22$) and mean $\delta^{13}C_s = +12.3 \pm 0.5$ ‰ (1σ, $n = 22$).

BGD
12, 13427–13481, 2015

Title Page
Abstract Introduction
Conclusions References
Tables Figures
◂ ▸
Back Close
Full Screen / Esc
Printer-friendly Version
Interactive Discussion

6 Discussion

6.1 Modern isotope data

Understanding how the isotope composition of contemporary lakewater relates to the measured signal from a mineral precipitate is fundamental in resolving the past systematics of hydroclimate variation from lacustrine records (Leng and Marshall, 2004). The isotope composition of present-day waters from Lake Ohrid, Lake Prespa and spring inflows have been previously investigated (Eftimi and Zoto, 1997; Anovski et al., 2001; Matzinger et al., 2006a; Leng et al., 2010a, 2013). The datasets cover water samples collected between 1984 to 2011 (summarised in Fig. 4), which show modern waters from Lake Ohrid fall on a Local Evaporation Line (LEL) away from the Local Meteoric Water Line (LMWL) inferring that they have undergone kinetic fractionation (Leng and Marshall, 2004). Lake Prespa has a reduced surface area to volume ratio in comparison to Ohrid, and is highly sensitive to seasonal variations in moisture balance due to the dominance of shallow groundwater (Popovska and Bonacci, 2007; Leng et al., 2010a), hence its waters fall higher on the LEL. In contrast, Lake Ohrid has a generally less variable and lower average isotope composition than Prespa. The initial water composition at the LMWL-LEL intersect suggests that both lakes are principally recharged from meteoric groundwater, assumed to be similar to the mean annual $\delta^{18}O_p$ across the catchment ($\delta^{18}O_p = -10.2$ ‰ ; Anovski, 2001), which falls close to the average value for precipitation-fed spring waters (−10.1 ‰). The spring complexes are split between those with lower $\delta^{18}O$ (fed predominantly by isotopically depleted winter precipitation) and those with higher $\delta^{18}O$ (having an evaporated component). Mixing analysis at spring complexes primarily to the southeast of Ohrid indicates they receive up to 53 % of their incoming water budget from Prespa (Anovski et al., 2001; Eftimi et al., 2001; Matzinger et al., 2006a). These springs contribute 26 % of total input to Lake Ohrid (Matzinger et al., 2006b), however they only account for 58 % of subterranean outflow from Lake Prespa (Anovski, 2001); the other 42 % is thought to reach Lake Ohrid through subaquatic springs (Matzinger et al., 2006a). The subaerial

BGD
12, 13427–13481, 2015

Mediterranean climate since the Middle Pleistocene

J. H. Lacey et al.

and subaquatic springs deliver 53 % of Lake Ohrid's total inflow, and therefore a large proportion of water input will be seasonally variable as it is derived from Lake Prespa (fresher in winter and enriched during summer). Contemporary waters from Lake Ohrid have a typically uniform composition over the ca. 30 year sampling period, signifying that seasonal variations in the water contribution from Lake Prespa has little overall effect and that Lake Ohrid has reached a steady state (Leng et al., 2010a), probably due to Ohrid's large volume and long lakewater residence time. This suggests that, in combination with modern lakewater that is isotopically heavier than local meteoric water, changes in the isotope composition of lakewater ($\delta^{18}O_{lw}$) are principally driven by regional water balance and most likely represent lower frequency changes in climate.

6.2 Late glacial to Holocene isotope data

A 10 m core (Co1262), recovered from the western margin of Lake Ohrid at the "Lini" drill site (Fig. 1), has been analysed for $\delta^{18}O_c$ at high-resolution over the Late Glacial to Holocene (Lacey et al., 2014); the study is utilised here as a recent comparison for the longer-term reconstruction in combination with the modern water isotope data. Lacey et al. (2014) highlighted the significance of Lake Ohrid as a sensitive recorder of climate change and confirmed that Ohrid responds to regional changes in water balance over the Holocene. Core Co1262 has $\delta^{18}O_c$ ranging between –6.5 and –2.1 ‰, being higher following the Late Glacial to Holocene transition, reaching a minimum between approximately 9 and 7 ka, and subsequently undergoes a step-wise increase to present day values (Fig. 5). This pattern of $\delta^{18}O_c$ variability is similar to other lake sediment sequences from Greece (Lake Pamvotis; Frogley et al., 2001), Turkey (Lake Acıgöl; Roberts et al., 2001), and also in speleothem records from Israel (Soreq Cave; Bar-Matthews et al., 1999). A period of sustained moisture availability above that of present day values is recorded between 8 ka and 6.5 ka from Lake Acıgol (Roberts et al., 2001), which is likewise identified at Lake Pamvotis where higher lake levels are inferred by a reduction in the quantity of shallow water ostracod taxa (Frogley et al., 2001). The Soreq Cave speleothem record indicates a greater annual number of heavy rainstorms throughout the period 10 to 7ka, with rainfall estimated to have been up to twice that of present day (Bar-Matthews et al., 1997), and similarly early Holocene rainfall is calculated to have increased by around 20 % in central Anatolia (Jones et al., 2007). A wetter early Holocene is suggested by several other central-eastern Mediterranean records, such as that from Lake Pergusa (Zanchetta et al., 2007), Lake Van (Wick et al., 2003), Lake Zeribar (Stevens et al., 2001), and Lake Göhlisar (Eastwood et al., 2007). The transition to reduced moisture availability and a more arid climate in the late Holocene is correspondingly reflected across these records, as well as the Lake Ohrid Lini sequence, as a progressive shift to higher $\delta^{18}O_c$. Therefore, the Holocene calibration dataset confirms that Lake Ohrid $\delta^{18}O_c$ is primarily driven by regional changes in water balance during the current interglacial.

6.3 SCOPSCO DEEP site isotope data

6.3.1 Oxygen isotope composition of calcite

$\delta^{18}O_c$ is dependent on $\delta^{18}O_{lw}$ and the temperature of lakewater at the time of precipitation, assuming equilibrium conditions (Leng and Marshall, 2004). Sediment trap data from Lake Ohrid shows that calcite precipitation is seasonally induced, with up to three times more TIC formed during summer months in comparison to winter months (Matzinger et al., 2007). The precipitation of calcite is thought to be associated with increased temperatures and the photosynthetic removal of CO_2 within the epilimnion, providing there is sufficient supply of calcium (Ca^{2+}) and bicarbonate (HCO_3^-) ions, which are mainly sourced from spring inflows (Matzinger et al., 2006a). Aquatic productivity, and therefore calcite precipitation, occurs predominantly around 20 m water depth, where phytoplankton density is greatest and elevated chlorophyll *a* concentrations are observed (Stankovic, 1960; Matzinger et al., 2007; Patceva and Mitic, 2008). The production of phytoplankton in the lake reaches a maximum between June and August, during which the temperature of the main productivity zone (around 20 m water depth) ranges between approximately 12 to 22 °C (Stankovic, 1960). If the average

BGD
12, 13427–13481, 2015

temperature of the photic zone during summer months is approximately 18 °C (0–20 m water depth average temperature between June–August), and taking the average modern $\delta^{18}O_{lw}$ of ca. −3.5 ‰ (Fig. 4), the calculated $\delta^{18}O_c$ of contemporary calcite precipitation should be approximately −4.0 ‰, using the equation of O'Neil et al. (1969), or −4.4 ‰ using the Leng and Marshall (2004) expression of Kim and ONeil (1997). This is similar to the average $\delta^{18}O_c$ through the Holocene (−4.9 ‰) and to the most recent measurement of $\delta^{18}O_c$ (−4.5 ‰) from core Co1262 (Lacey et al., 2014), suggesting that $\delta^{18}O_c$ most likely corresponds to summer lakewater conditions.

Calcite may comprise up to around 80 % of the total sediment composition (assuming TIC mainly represents $CaCO_3$; Wagner et al., 2008), with only a minor biogenic component (< 0.1 %) and limited terrigenous contribution (Lézine et al., 2010). As Lake Ohrid is located within a karst catchment, a proportion of the carbonate could be of detrital origin, which commonly has a different isotope composition to the endogenic fraction (Leng et al., 2010b). The catchment geology has variable $\delta^{18}O$ (−9.7 to −2.6 ‰ ; Leng et al., 2010a), however SEM investigations have shown that the calcite crystals have mostly morphological characteristics (for example size and shape) typical of an endogenic origin (Lézine et al., 2010; Matter et al., 2010).

The modern isotope data from Lake Ohrid indicate a clear evaporative disparity between the isotope composition of lakewater and that from meteoric and ground water sources (Fig. 4). Modern precipitation measured at St. Naum has $\delta^{18}O_p$ = −8.4 ‰ (Anovski et al., 2001), and using the mean summer lakewater temperature (+18 °C), the calcite precipitated from a hypothetical, exclusively meteoric water source would have $\delta^{18}O_c$ = −8.9 ‰. Similarly low $\delta^{18}O_c$ are rarely seen in any isotope data produced from Lake Ohrid to date, including core catcher data covering the entire 1.2 Ma sediment sequence (Wagner et al., 2014), which indicates that lakewater has always been subject to a varying extent of evaporative fractionation. This assumes that $\delta^{18}O_{lw}$ is largely not influenced by changes in $\delta^{18}O_p$ or temperature, and that $\delta^{18}O_{lw}$ is primarily influenced by long-term changes in the precipitation/evaporation ratio (P/E; Leng and Marshall, 2004; Leng et al., 2010a). If, however, lakewater temperature were the dominant influence on $\delta^{18}O_c$, the change displayed between modern (−4.5 ‰) and early Holocene (−6.5 ‰) values in Co1262 (Lacey et al., 2014) would require a decrease of over 5 °C from that of present day (as the measured carbonate will covary with temperature by +0.36 ‰ °C^{-1}; Leng and Marshall, 2004). The early Holocene is characterised by the presence of thermophilous arboreal taxa within the catchment area (Panagiotopoulos et al., 2013) and generally stable, warm climate conditions (Bordon et al., 2009), suggesting that such a significant temperature drop is unlikely and indicates that temperature has a negligible direct influence on $\delta^{18}O_c$, at least during the current interglacial.

The $\delta^{18}O_c$ data from calcite in Lake Ohrid is restricted to the interglacial (or interstadial) periods. Interglacial sediments are characterised by concomitant increases in both TIC and TOC (Francke et al., 2015), suggested to be the result of enhanced primary productivity associated with a warmer climate (Wagner et al., 2010). Calcite precipitation is favoured by elevated temperatures during interglacials, which drives higher evaporation rates, thereby concentrating Ca^{2+} and HCO_3^- ions. Further, enhanced moisture availability delivers more dissolved ions through karst spring water and warmer surface waters lower the calcite saturation threshold (Lézine et al., 2010). Conversely, glacial sediments typically have low TIC/TOC that anti-correlate with K and Ti profiles, indicating low productivity and increased clastic input (Vogel et al., 2010). Lower temperatures during glacial periods would lead to a more oxygenated water column through increased vertical mixing and more frequent complete deep convective overturn. Enhanced levels of mixing breaks down water column stratification and associated oxygenation of the water column increases the rate of aerobic decomposition of organic matter, releasing CO_2 that reduces pH levels and increases calcite dissolution (Vogel et al., 2010). Following extensive organic matter degradation, the C/N ratio of sediments may be significantly reduced, as observed in a previous core from Lake Ohrid where during the Last Glacial C/N values were typically very low (4–5) compared to higher values (8–12) in both the Holocene and MIS 5 (Leng et al., 2010a). Catchment permafrost may have also been prevalent in glacial periods, limiting the supply of Ca^{2+}

and HCO_3^- ions to the lake by reducing the volume of karstic spring inflow (Belmecheri et al., 2009), which is supported by pollen-inferred mean annual temperatures during the Late Glacial of between −3 and +1 °C (Bordon et al., 2009). Although there is no (or limited) calcite in the glacial periods, previous work on Lake Ohrid has shown spikes in TIC during MIS 2–3 (Wagner et al., 2010), and similar increases in glacial TIC are observed throughout the 5045-1 composite profile (Francke et al., 2015). These TIC spikes are most likely analogous to those found in Lake Prespa glacial sediments during MIS 4–2, which comprise siderite (Leng et al., 2013).

6.3.2 Oxygen isotope composition of siderite

Within the Lake Ohrid record, multiple siderite-bearing horizons have been identified from visual core description and XRF results (Francke et al., 2015). The presence of siderite has subsequently been confirmed using XRD and FTIRS, and its morphology and geochemistry investigated using SEM-EDX. Thin sections from discrete higher TIC glacial intervals reveal individual siderite crystals (ca. 5 µm) and siderite crystal clusters (ca. 50–100 µm) nucleating within an uncompacted clay matrix (Fig. 6). The distribution of siderite within each thin section is variable; a higher concentration of siderite crystals is contained within burrow-like structures that impart a mottled texture to the sediment. Occasional dolomite grains, large (> 20 µm) and distinct from the fine clay matrix, are fringed by 5 µm grains of siderite. Siderite comprises the principal carbonate component in these horizons, and apart from the occasional dolomite crystals, no other type of carbonate has been observed. The dolomite crystals are thought to be detrital as they are larger than the individual siderite grains, and have irregular margins. Individual siderite crystals appear to predominantly form within the open framework of the clay matrix, which suggests they precipitated in situ within the available pore space and are therefore likely to be early diagenetic formed before compaction within the sediment. Authigenic siderite has been observed to precipitate in porewaters close to the sediment–water interface from dissolved ferrous iron (Fe^{2+}) and carbonate ions (Wersin et al., 1991; Lebeau et al., 2014). Siderite is generally formed under anoxic and

BGD
12, 13427–13481, 2015

reducing conditions, which typically have a high CO_2 partial pressure, elevated Fe/Ca and a low sulphide concentration (Bahrig, 1988; Brauer and Negendank, 1993). The availability of dissolved Fe^{2+} for siderite formation is determined by the oxygen and sulphide content of the porewater, as Fe^{2+} is readily oxidised to Fe^{3+} in the presence of molecular oxygen, and will preferentially react with H_2S to produce iron sulphide (Coleman, 1985; Lebeau et al., 2014). Thusly, siderite precipitation is most likely a function of the environmental setting and is dependent on the presence of redox-sensitive elements, which are influenced by changes in water column stratification that may vary seasonally (Balistrieri et al., 1992) as well as on a centennial to millennial scale (Katsuta et al., 2006). Discrete horizons enriched in Fe have been previously observed in Lake Ohrid (Vogel et al., 2010), neighbouring Lake Prespa (Wagner et al., 2010; Leng et al., 2013), and in other ancient lakes, such as Lake Baikal (Granina et al., 2004), where the formation of Fe-enriched layers up to approximately 25 cm below the sediment–water interface is thought to be related to bottom water redox conditions and significant changes in sedimentation regime. Assuming the siderite is formed in superficial sediments during the initial stages of diagenesis, like calcite, its isotope composition can be used as an indicator of depositional environment (Mozley and Wersin, 1992).

6.3.3 Comparison of $\delta^{18}O_c$ and $\delta^{18}O_s$

The $\delta^{18}O$ of siderite (and calcite) is a function of both $\delta^{18}O_{lw}$ and the temperature of lakewater during precipitation; however, $\delta^{18}O_s$ and $\delta^{18}O_c$ cannot be directly compared due to different mineral-water fractionations and formation temperatures (Leng et al., 2013). Though the temperature-dependent oxygen isotope fractionation between calcite and water has been extensively studied (e.g. Epstein et al., 1953; Craig, 1965; O'Neil et al., 1969), there are fewer studies into the siderite-water fractionation (Becker and Clayton, 1976; Carothers et al., 1988; Zhang et al., 2001) and published fractionation equations for siderite-water differ significantly at low temperatures (Krylov et al., 2008). Ludvigson et al. (2013) show that in pedogenic siderites, the fractionation equations of Carothers et al. (1988) and Zhang et al. (2001) diverge below +30 °C, and that the equation of Zhang et al. (2001) is more appropriate for defining equilibrium precipitation at lower temperatures.

To enable comparison between calcite and siderite and their respective $\delta^{18}O$ composition, we convert both $\delta^{18}O_c$ and $\delta^{18}O_s$ to $\delta^{18}O_{lw}$ using specific mineral fractionation equations and different estimates of temperature (after Leng et al., 2013). For interglacial intervals (calcite data), we use the equation of O'Neil et al. (1969) and a precipitation temperature of +18 °C to represent average summer conditions within the photic zone during the period of maximum phytoplankton activity. During glacial intervals (siderite data), we use the equation of Zhang et al. (2001), and assume a bottom water temperature of +5.8 °C (average temperature measured during 1932–1951 at water depths between 250–285 m; Stankovic, 1960). The calculated $\delta^{18}O_{lw}$ for calcite and siderite using their respective fractionation equation and formation temperature are given in Fig. 3 and the averages for each MIS are compared to those of $\delta^{13}C_c$ and $\delta^{13}C_s$ in Fig. 7a.

The modelled $\delta^{18}O_{lw}$ from siderite are generally lower than those calculated for calcite, which suggests that the siderite-bearing horizons were formed when Lake Ohrid was isotopically fresher, in comparison to higher $\delta^{18}O_{lw}$ during warmer interglacial periods (Fig. 7). Although siderite horizons probably represent distinct rapid and recurrent events in Lake Ohrid (Vogel et al., 2010), overall lower $\delta^{18}O_{lw}$ is nevertheless expected through glacial periods due to reduced lakewater evaporation as a result of decreased temperatures. Jones et al. (2007) calculated evaporation rates at Eski Acıgöl in central Turkey, and showed that glacial evaporation was around 3 times lower compared to that of the Late Holocene ($0.4\,m\,yr^{-1}$ vs. $1.1\,m\,yr^{-1}$). If a similar calculation is conducted for Lake Ohrid, glacial evaporation may have been over 4 times lower than during the present interglacial ($0.4\,m\,yr^{-1}$ vs. $1.8\,m\,yr^{-1}$), after Jones et al. (2007) using the equation of Linacre (1992). Higher evaporation rates are typically associated with closed lake basins and covariance between $\delta^{18}O$ and $\delta^{13}C$ (Talbot, 1990; Li and

BGD
12, 13427–13481, 2015

Ku, 1997), which is observed in the Lake Ohrid data as interglacial $\delta^{18}O_{lw}$ from calcite ($r_c = 0.30$) has a higher covariance than glacial $\delta^{18}O_{lw}$ from siderite ($r_s = 0.16$; Fig. 7b), corroborating that evaporation was stronger during interglacials. As rates of evaporation reduce, the influence of other controlling factors, such as $\delta^{18}O_p$, may have had a greater importance in determining $\delta^{18}O_{lw}$ during glacial periods.

During colder intervals, $\delta^{18}O_p$ would have been lower as a direct correlation exists between annual precipitation and temperature, where $\delta^{18}O_p$ is reduced by roughly −0.6 ‰ for every 1 °C drop in temperature at mid-high latitudes (Dansgaard, 1964). If a mean annual temperature difference of up to 9 °C is assumed between interglacial and glacial periods, based on pollen-inferred temperature data from nearby Lake Maliq (Bordon et al., 2009), $\delta^{18}O_p$ would decrease by –5.4 ‰ in glacial periods. However, when considering interglacial–glacial timescales, changes to the oxygen isotope composition of seawater ($\delta^{18}O_{sw}$; the main source of atmospheric moisture) must also be considered, as ^{16}O is preferentially stored in polar ice causing glacial oceans to have higher $\delta^{18}O_{sw}$. North Atlantic and Adriatic planktonic foraminifera indicate a $\delta^{18}O$ increase of around +3 ‰ during glacial periods (McManus, 1999; Siani et al., 2010), which will itself be partially counteracted by a temperature dependent fractionation during carbonate precipitation. The resultant net effect of temperature and source $\delta^{18}O_{sw}$ changes during glacial periods is therefore thought to produce lower $\delta^{18}O_p$.

In addition to more regional effects on $\delta^{18}O_{lw}$, local influences may also contribute to lower isotope values through glacial periods. Today, a significant proportion of winter precipitation occurs as snowfall at higher altitudes in the Ohrid-Prespa catchment, which is ultimately transferred to the lakes during spring when temperatures remain high enough for the snow to melt (Hollis and Stevenson, 1997; Popovska and Bonacci, 2007). Average winter temperatures at present are around 2 °C (Stankovic, 1960), however winter temperature would have been considerably reduced during glacial periods and temperature during summer months may also have been lower (Bordon et al., 2009). If lower temperatures persisted throughout much of the year, a higher propor-

BGD
12, 13427–13481, 2015

Mediterranean climate since the Middle Pleistocene

J. H. Lacey et al.

tion of annual precipitation may have fallen in winter as snow. Snow is typically characterised as having much lower $\delta^{18}O$ than rainfall, which reflects in-cloud equilibrium conditions and cooler condensation temperatures (Darling et al., 2006), and so would provide a further potential source for low $\delta^{18}O$.

Temperatures may have been sufficiently reduced during glacials to also allow (at least discontinuous) permafrost to form in the Ohrid catchment, thereby decreasing input from karst waters and perhaps restricting the inflow of water from Lake Prespa (Belmecheri et al., 2009). Lake Prespa provides a large proportion of water input to Ohrid through the underground network of karst channels, which has higher $\delta^{18}O_{lw}$ when compared to measured precipitation (Fig. 4; Leng et al., 2010a, and references therein). This infers that during periods where glacial conditions were prevalent in the catchment, the inflow of water comprising high $\delta^{18}O$ from Lake Prespa may have reduced, and input would have instead been principally sourced from a combination of direct precipitation and surface run-off, both of which would result in lower $\delta^{18}O_{lw}$. A scenario of enhanced surface run-off is further supported by an increase in the amount of fine sand found in sediments during corresponding intervals in the Last Glacial and concomitant increases in Zr/Ti and Cr/Ti ratios, thought to be proxies for catchment erosion rates (Vogel et al., 2010).

6.3.4 Carbon isotope composition of carbonate

When a carbonate mineral precipitates under equilibrium conditions, as with $\delta^{18}O$, it captures the $\delta^{13}C$ of the total dissolved inorganic carbon (TDIC) of lakewater, which for most lakes (at a neutral pH) can be approximated to HCO_3^-. Dissolved HCO_3^- is principally derived from the dissolution of carbonate catchment rocks, soils and atmospheric CO_2 (Leng et al., 2013); consequently, there are several carbon reservoirs that may contribute to the overall carbon budget of a lake (Cohen, 2003). In a lacustrine environment, $\delta^{13}C_{TDIC}$ is influenced by multiple factors including the $\delta^{13}C$ of inflowing waters and by two predominant fractionation effects: (1) the chemical exchange between atmospheric CO_2 and dissolved HCO_3^-, and (2) kinetic processes during the formation of organic matter (Hoefs, 1980; McKenzie, 1985). In Lake Ohrid, endogenic calcite precipitated within the epilimnion is thought to form in equilibrium with surface waters, thus $\delta^{13}C_c$ can provide information on past variations in $\delta^{13}C_{TDIC}$ and associated carbon-cycle transitions (Leng and Marshall, 2004). The DEEP site record (Fig. 3) shows overall high and consistent $\delta^{13}C_c$ throughout the core (+0.4 ± 0.6 ‰, 1σ, $n = 924$), which is most likely driven in part by the inflow $\delta^{13}C$, especially that pertaining to the spring network. In areas with karst aquifers the local and groundwater chemistry will be dominated by Ca^{2+} and HCO_3^- ions (Cohen, 2003), and $\delta^{13}C_{TDIC}$ will be high as catchment limestones usually comprise ancient marine carbonates that, by definition, have average $\delta^{13}C$ around 0 ‰ (Hudson, 1977; Jin et al., 2009), and typically range between −3 and +3 ‰ (Andrews et al., 1993; Hammarlund et al., 1997). Although $\delta^{13}C_{TDIC}$ has not been measured for Lake Ohrid, analysis conducted on several of the main geological units in the catchment provides average $\delta^{13}C$ of +1 ‰ (Leng et al., 2010a), which confirms that $\delta^{13}C_{TDIC}$ will most probably be high as over 50 % of water input to Ohrid is derived from springs fed by karst aquifers (Matzinger et al., 2006b). Over glacial–interglacial timescales, the extent to which geological sources of carbon contribute to TDIC will primarily be determined by hydrological balance and associated changes in the residence time of water passing through the karst system; lower $\delta^{13}C_{TDIC}$ may occur during wetter periods with a lower residence and higher $\delta^{13}C_{TDIC}$ in more arid periods with a higher residence time.

In opposition to geological sources of high $\delta^{13}C$, a major source of carbon in ground and river water typically derives from isotopically light CO_2 liberated during the decay of terrestrial organic matter. Low $\delta^{13}C_{TDIC}$ are shown in isotope data from Lake Prespa springs and rivers that have average $\delta^{13}C_{TDIC}$ of −11.5 ‰ (Leng et al., 2013), which is consistent with the calculated range for a soil CO_2-derived carbon source (−22 to −10 ‰ for C3 plants; Leng and Marshall, 2004) and may also be similar to the river inflow into Lake Ohrid (forming 23 % of overall water input; Matzinger et al., 2006b). Over glacial–interglacial timescales, variations in the proportion of soil-derived CO_2, in addition to a differing contribution from C3 and C4 sources, are likely to influence $\delta^{13}C_{TDIC}$.

BGD
12, 13427–13481, 2015
Mediterranean climate since the Middle Pleistocene
J. H. Lacey et al.

In colder periods $\delta^{13}C_{TDIC}$ would have increased as catchment soil development was poor due to a prevalent open landscape comprising temperate trees (Panagiotopoulos et al., 2014). Whereas, during warmer intervals, denser forests dominated by deciduous trees became established producing well-developed soils that would act to lower $\delta^{13}C_{TDIC}$ and encourage the delivery of Ca^{2+} and HCO_3^- through the dissolution of carbonate catchment rocks.

Lake Ohrid is known to lose a proportion (34 %) of water through evaporation (Matzinger et al., 2006b) and modern lakewater sits on a LEL away from the LMWL (Fig. 4), which suggests Ohrid is sensitive to moisture balance. This indicates a degree of hydrological closure and is consistent with Ohrid's long residence time of approximately 70 years. Isotope exchange between TDIC and atmospheric CO_2 is more likely to occur in a standing body of water (closed lakes), and if enough time is available the exchange process will tend toward equilibrium (Usdowski and Hoefs, 1990). Equilibrium exchange between atmospheric CO_2 and lakewater will result in aqueous TDIC with $\delta^{13}C$ of around +3 ‰ (fractionation factor +10 ‰ when in equilibrium with CO_2 gas). Therefore, as $\delta^{13}C_c$ is thought to reflect changes in $\delta^{13}C_{TDIC}$, higher $\delta^{13}C_c$ in the Ohrid record may reflect variable degrees of equilibration between atmospheric CO_2 and aqueous HCO_3^-. This process is also observed in isotope data from Lake Prespa, where low $\delta^{13}C_{TDIC}$ entering the lake (−11.5 ‰) is modified by within-lake processes to increase lakewater $\delta^{13}C_{TDIC}$ to give the average value of −5.2 ‰ (Leng et al., 2013). In addition to evaporation, it is also likely that biogenic productivity drives higher $\delta^{13}C_{TDIC}$ in Prespa (and Ohrid) due to the preferential incorporation of ^{12}C during photosynthesis, thus leaving TDIC isotopically heavy assuming the organic carbon is exported to the lake floor and buried (Meyers and Teranes, 2001). Therefore, particularly in warmer climate conditions, Lake Ohrid will become isotopically enriched through evaporative processes and/or biological productivity and so will a major component of its inflow, as Lake Prespa $\delta^{13}C_{TDIC}$ concurrently tends toward heavier values.

Evaporative drawdown in closed lakes or long residence time lakes, such as Ohrid, will also affect $\delta^{18}O$ as the preferential loss of ^{16}O during evaporation can drive ^{18}O-enrichment resulting in covariance between $\delta^{18}O$ and $\delta^{13}C$. The signal of covariance will be recorded in primary lacustrine carbonates and can potentially be used to determine the degree of past hydrological closure (Talbot, 1990). The extent to which isotope measurements covary can depend of several factors, including hydrological balance, stability of the lake volume, vapour exchange and evaporation (Li and Ku, 1997). Covariance may therefore not simply be a function of residence time or hydrological closure (Leng et al., 2010a), and has been shown to be spatially inconsistent between Mediterranean lake sediment records (Roberts et al., 2008). Nevertheless, major lake level fluctuations are thought to have occurred in Lake Ohrid, at least during MIS 6, as evidenced by the presence of subaquatic terraces on the northeast shore of the lake (Lindhorst et al., 2010). Significant reductions in lake level, most probably coincident with periods of regional aridity and generally lower P/E, may limit surface outflow, solely met at present by the river Crn Drim (66 %; Matzinger et al., 2006b), which in turn would extend lakewater residence time and increase the possibility of evaporation, isotope exchange and covariance, driving $\delta^{18}O$ and $\delta^{13}C$ to higher values. However, periods of higher covariance are generally restricted to certain intervals, for example MIS 5 ($r = 0.53$, $p = < 0.001$, $n = 104$), as throughout the whole core correlation between $\delta^{18}O$ and $\delta^{13}C$ is generally weak ($r = 0.30$, $p = < 0.001$, $n = 924$; Fig. 7). In those areas where $\delta^{18}O$ and $\delta^{13}C$ are decoupled, local in situ process are likely to dominate the evolution of $\delta^{13}C_{TDIC}$ and act to buffer any climate signal (Regattieri et al., 2015).

In contrast to $\delta^{13}C_c$, $\delta^{13}C_s$ is higher in Lake Ohrid sediments by at least +8 ‰, and has a mean value of +12.3±0.5 ‰ (1σ, $n = 22$). Higher $\delta^{13}C$ is characteristic of siderite formed in non-marine sediments and is most probably associated to the incorporation of ^{13}C-enriched bicarbonate derived from methanogenesis. As lacustrine environments generally contain low sulphate concentrations, any sulphate that is present will rapidly become reduced at shallower levels in the sediment leaving more organic matter for methanogenic decomposition by bacteria (Mozley and Wersin, 1992). The metabolic pathway utilised by bacteria during the reduction of organic matter strongly fractionates in favour of light carbon (^{12}C), which, for isotopic mass balance, produces isotopically light methane and proportionally enriches the bicarbonate ion in ^{13}C. The methane is subsequently removed by ebullition or by emission through the stems of aquatic macrophytes, and the enriched bicarbonate is incorporated into TDIC (Curry et al., 1997). Methanogenic bicarbonate is therefore the probable source of carbon for the isotopically heavy siderite.

6.4 Climate and interglacial variability at Lake Ohrid over the past 640 ka

The Late Quaternary is characterised by cyclic alternations between colder glacial and warmer interglacial periods, the timing and magnitude of which are principally determined by orbital-induced climate oscillations and variations in atmospheric greenhouse gas content (Imbrie et al., 1984; Shackleton, 2000). This glacial–interglacial climate signal has been globally observed in deep marine sediments (Lisiecki and Raymo, 2005), ice cores (Jouzel et al., 2007), and continental sequences (Sun and An, 2005), which, when compared, indicate a broad correspondence over orbital timescales (Tzedakis et al., 1997; Lang and Wolff, 2011). However, in opposition to numerous oceanic records, extended high resolution continental sequences are still rare (Prokopenko et al., 2006; Tzedakis et al., 2006), especially when isotope stratigraphies are considered, and consequently the Lake Ohrid 5045-1 sequence can provide valuable information on climate trends over an extended timeframe. While glacial $\delta^{18}O_{lw}$ is made available by the analysis of authigenic siderite, the dataset is at low resolution and so comparison between glacial periods is not yet achievable. However, higher resolution interglacial $\delta^{18}O_{lw}$ calculated from calcite enables a more robust measure of variability and assessment of changing climate dynamics through the Late Quaternary (Fig. 8). Although it is beyond the scope of this paper to look in detail at each of the interglacials over the last 640 ka (MIS 15 to MIS 5), some preliminary observations can be made about their structure and consistency.

BGD
12, 13427–13481, 2015

6.4.1 MIS 16-13 (640–478 ka)

At the transition between MIS 16 and 15, $\delta^{18}O_{lw}$ increases from relatively low values to higher values following a peak, concomitant with increasing TIC and biogenic silica (BSi; Francke et al., 2015), which suggests a gradual warming and increasing evaporation of lakewater (lower P/E) following the MIS 16 glacial. The positive $\delta^{18}O_{lw}$ excursions within MIS 15, centred on ca. 618, 586, and 567 ka, are most likely related to negative $\delta^{18}O$ excursions in LR04 (Fig. 8; Lisiecki and Raymo, 2005), the Mediterranean Sea (Kroon et al., 1998) and the Ionian Sea (Rossignol-Strick and Paterne, 1999), representing an influx of glacial meltwater into the oceans and warmer conditions during MIS 15e, 15c, and 15a. In addition, this is mirrored by high arboreal pollen (AP) at Tenaghi Philippon (Tzedakis et al., 2006) and warmer temperatures during these times would have promoted enhanced evaporation at Lake Ohrid, leading to lower P/E and higher $\delta^{18}O_{lw}$.

Following MIS 15, MIS 14 is the only glacial of the record to contain a higher proportion of TIC throughout the majority of the stage, indicating temperatures at Lake Ohrid did not decrease significantly to abate calcite production, and thus isotope data is available for MIS 14. Hydroclimate conditions are assumed to have remained fairly similar to MIS 15 as average $\delta^{18}O_{lw}$ remains consistent between the two stages, suggesting that MIS 14 was a particularly weak glacial. Prolonged warming through MIS 14 is in agreement with a range of global records, including in sea surface temperature estimates from the Iberian margin (Fig. 8; Rodrigues et al., 2011) and South China Sea (Yu and Chen, 2011), BSi and magnetic susceptibility from Lake Baikal (Prokopenko et al., 2002, 2006), and several proxies from Antarctic ice cores (Jouzel et al., 2007; Masson-Delmotte et al., 2010). Although full interglacial conditions may have persisted during MIS 14, the Ohrid record suggests that colder glacial conditions occurred between ca. 541 ka to 533 ka, where there is a distinct decrease in TIC (Francke et al., 2015). A single $\delta^{18}O_{lw}$ data point for this interval is considerably higher than surrounding values, which is most likely due to a mixing of carbonate sources through the cold glacial phase of MIS 14, as siderite is present at this time (Fig. 3).

MIS 13 in the Lake Ohrid $\delta^{18}O_c$ record represents a relatively stable interglacial, experiencing only minor oscillations for most of the stage, with average $\delta^{18}O_{lw}$ equal to that of MIS 14 and 15. However, although appearing similar to MIS 15 (and MIS 14) in Lake Ohrid, MIS 13 is generally considered to be the weakest interglacial of the last 800 ka (Lang and Wolff, 2011). The negative excursion centred around ca. 510 ka is probably linked to cooler conditions during MIS 13b and higher P/E, which is similar to observations from Tenaghi Philippon and Antarctic ice cores that indicate lower AP and reconstructed temperatures (Tzedakis et al., 2006; Jouzel et al., 2007). LR04 that exhibits higher $\delta^{18}O$ at this time signifying an expansion of global ice volume (Fig. 8; Lisiecki and Raymo, 2005). MIS 13a $\delta^{18}O_{lw}$ are slightly elevated above those of MIS 13c, which suggests the latter may have had marginally higher P/E due to cooler conditions or higher annual precipitation. Within the LR04 isotope stack, an excursion to lighter $\delta^{18}O$ occurs in MIS 13a beyond that of the shift seen during MIS 13c (Lisiecki and Raymo, 2005), which is also observed in the Ionian Sea (Rossignol-Strick and Paterne, 1999), and at the same time as higher reconstructed temperatures and atmospheric CO_2 and CH_4 recorded in Antarctic ice cores (Fig. 8; Jouzel et al., 2007; Loulergue et al., 2008). Peaks to higher $\delta^{18}O_{lw}$ toward the end of MIS 13 are coincident with an increased proportion of siderite in sediments (Fig. 3), and so may have been artificially enhanced rather than representing a period of lower P/E.

6.4.2 MIS 11 (424–374 ka)

MIS 11 is thought to have a characteristic orbital and climate configuration potentially analogous to that of the Holocene, and may be of great importance to the understanding and prediction of future climate scenarios (Loutre and Berger, 2003). The stage is also suggested to be the longest interglacial of the Late Quaternary (McManus, 1999), and the strongest interglacial in several temperature reconstructions from both the Northern and Southern Hemispheres (Lang and Wolff, 2011). At Lake Ohrid, the $\delta^{18}O_{lw}$ record shows a general trend of low and then increasing values up to ca. 400 ka, followed by a decline to a minimum $\delta^{18}O_{lw}$ toward the end of the stage. The relatively negative $\delta^{18}O_{lw}$ at the inception of MIS 11 are similar to values observed during other terminations and through glacial periods, and can be traced from lower $\delta^{18}O_{lw}$ (calculated from siderite) in MIS 12 that display an increasing trend toward the start of MIS 11. The lower $\delta^{18}O_{lw}$, as well as an absence of TIC until around ca. 420 ka, suggest that MIS 11e is not overly distinct from MIS 12 and warmer conditions did not perhaps become pervasive at Lake Ohrid until MIS 11c. The $\delta^{18}O_{lw}$ increase at the beginning of MIS 11c shows a short-lived reversal to lower $\delta^{18}O_{lw}$ at ca. 410–408 ka, implying higher P/E, a short term deterioration in climate and cooler conditions. A characteristic short-term reversal during early MIS 11 is also overserved in atmospheric CH_4 (Loulergue et al., 2008), which is coincident with reduced sea surface temperatures at the western Iberian Margin (Fig. 8; Martrat et al., 2007; Rodrigues et al., 2011) and in the North Atlantic (Stein et al., 2009). However, the short-term excursion in these records is found earlier between 415–412 ka and is likely associated with the stadial MIS 11d. This may suggest that higher $\delta^{18}O_{lw}$ at Ohrid around 415 ka are actually related to MIS 11e, at the lower values around 410 ka are actually concomitant with MIS 11d. Evaporating lakewater conditions at Lake Ohrid (MIS 11 maximum $\delta^{18}O_{lw}$ occur around ca. 402 ka) are broadly synchronous with a significant drop in the water level of Lake Amora (Dead Sea basin; Torfstein et al., 2009), low surface $\delta^{18}O$ in the Ionian Sea (Rossignol-Strick and Paterne, 1999), and elevated global atmospheric CO_2 and CH_4 contents (Fig. 8; Petit et al., 1999; Loulergue et al., 2008). Transitioning to MIS 11b, and throughout MIS 11a, $\delta^{18}O_{lw}$ become progressively lower until reaching a minimum at the boundary with MIS 10 and after which TIC is absent. The trend to lower $\delta^{18}O_{lw}$ in the second half of MIS 11 displays greater variability in comparison to the first, suggesting that the stability of hydroclimate conditions changed as temperature assumedly reduced after the peak interglacial. Greater variability after ca. 400 ka is also seen in other proxies from Lake Ohrid (TIC, BSi; Francke et al., 2015), and also in reconstructed SST at the Iberian Margin (Rodrigues et al., 2011) and atmospheric CH_4 and temperature profiles from Antarctic ice cores (Fig. 8; Petit et al., 1999; Jouzel et al., 2007).

6.4.3 MIS 9 (337–300 ka)

The initial ca. 5 ka of MIS 9 is marked by a transition from lower to higher $\delta^{18}O_{lw}$, similar to previous interglacial stages, however this may be related here to increased precipitation and higher P/E. If warming was abrupt at the start of MIS 9, as seen in AP from Tenaghi Philippon (Tzedakis et al., 2006) and SST from the Iberian Margin (Fig. 8; Martrat et al., 2007), greater initial precipitation could have preceded enhanced evaporation during later stages of MIS 9e. The $\delta^{18}O_{lw}$ peak at ca. 324 ka is considered to represent the warmest and most evaporative conditions of MIS 9, with the higher values around ca. 318 ka being related to a climate cooling coincident with a low TIC interval (Francke et al., 2015) and a distinct minima in AP at Tenaghi Philippon (Fig. 8; Tzedakis et al., 2006) during MIS 9d. The following transition to lower $\delta^{18}O_{lw}$ around ca. 310 ka is probably associated with a warmer climate, higher precipitation and P/E during MIS 9c, reflected at Tenaghi Philippon by higher AP and moderately lower $\delta^{18}O$ in the LR04 stack (Fig. 8). In general $\delta^{18}O_{lw}$ during MIS 9 has the lowest average values of the calcite record (Fig. 7), particularly when “MIS 8” data are included; $\delta^{18}O_{lw}$ data between ca. 291 and 281 ka are identified to be part of MIS 8 under certain classifications (Bassinot et al., 1994; Lisiecki and Raymo, 2005), however are designated as MIS 9a in others (Tzedakis et al., 1997; Railsback et al., 2015). The data are separated from the main body of MIS 9 $\delta^{18}O_{lw}$ by a ca. 15 ka zone of low TIC (Francke et al., 2015), which is assumed to correspond to MIS 9b and represent a return to colder, less evaporated conditions as the bounding $\delta^{18}O_{lw}$ values are low and siderite is present (Fig. 3). Whether the short-lived warming around ca. 286 ka belongs to MIS 8 or MIS 9 may remain controversial, however the presence of siderite infers that MIS 9b most likely experienced glacial-like conditions at Lake Ohrid. Overall, low $\delta^{18}O_{lw}$ through the

BGD
12, 13427–13481, 2015

majority of MIS 9 are coincident with similarly low values for glacial lakewater, where glacial and interglacial $\delta^{18}O_{lw}$ appear to broadly converge.

6.4.4 MIS 7 (243–191 ka)

MIS 7 at Lake Ohrid is characterised by three distinct phases of calcite preservation (Francke et al., 2015), which probably correspond to MIS sub-stages 7e, 7c and 7a (Fig. 3; Railsback et al., 2015, and references therein). The first peak in TIC between ca. 244 and 236 ka is associated with initially low $\delta^{18}O_{lw}$ that steadily increase over the next ca. 8 ka. The increasing $\delta^{18}O_{lw}$ suggest that climate conditions at Ohrid became more evaporating through this interval and P/E reduced, which is coincident with warming indicated by arboreal expansion at the Ioannina (Roucoux et al., 2008) and Tenaghi Philippon (Fig. 8; Tzedakis et al., 2006) basins in Greece and at Lake Van in Turkey (Litt et al., 2014). In addition, higher SST are observed at this time in the Adriatic Sea (Piva et al., 2008) and on the Iberian Margin (Fig. 8; Martrat et al., 2007). Following a cessation of TIC production indicating a colder, glacial-like climate during stadial MIS 7d, $\delta^{18}O_{lw}$ is low and has similar values to the start of MIS 7e after what is assumed to be a return to glacial-like conditions through MIS 7d. After ca. 220 ka there is a sharp rise in TIC associated with a step-wise $\delta^{18}O_{lw}$ increase through to ca. 212 ka, at which point a maximum is reached. This is beyond the upper extent of $\delta^{18}O_{lw}$ values in the previous sub-stage (MIS 7e), which is generally considered to represent the full interglacial as MIS 7e had the highest atmospheric CO_2 and CH_4 content of the MIS from Antarctic ice cores (Fig. 8; Petit et al., 1999; Loulergue et al., 2008). The Ohrid record suggests that during MIS 7c the lake experienced generally more evaporated conditions than in MIS 7e, although several short-term reversals to colder conditions do interrupt the sequence. Many other records also indicate that MIS 7c experienced full interglacial conditions either equal to or superseding MIS 7e, such as at Tenaghi Philippon where a greater diversity of arboreal pollen is observed along with a higher

BGD
12, 13427–13481, 2015

abundance of thermophilous taxa (Tzedakis et al., 2003b) and at Lake Baikal higher percentages of BSi are found within MIS 7c (Prokopenko et al., 2006).

A proportion of the highest $\delta^{18}O_{lw}$ of the stage are observed between ca. 206 and 204 ka, however a spike in siderite concentration also occurs at this time meaning that a mixture of carbonate sources may have been analysed. Although, the presence of siderite may indicate that a rapid temperature decrease occurred and that a short-lived return to glacial conditions resulted in lower TIC and BSi (Francke et al., 2015). This interval is coincident with MIS 7b (Railsback et al., 2015) and occurs at a similar time to a decline in arboreal pollen percentages at Lake Van (Litt et al., 2014) and Tenaghi Philippon (Tzedakis et al., 2003b). However, these records indicate that MIS 7b experienced more temperate conditions when compared to MIS 7d, which is corroborated by the Ohrid record as $\delta^{18}O_{lw}$ remains stable through much of the stadial interval characterised by lower (> 1 %) TIC, whereas in MIS 7d TIC (and therefore isotope data) becomes absent. MIS 7a in Lake Ohrid is short-lived and characterised by a shift to lower $\delta^{18}O_{lw}$, in comparison to MIS 7c following the stadial phase, that are highly variable but overall increase until TIC production ceases at around ca. 200 ka. An increase in the extent of $\delta^{18}O_{lw}$ variability through MIS 7a suggests a change in hydroclimate stability, which is also reflected in the Tenaghi Philippon pollen record (Tzedakis et al., 2003b), and in $\delta^{18}O$ of speleothems from the Peqiin Cave, northern Israel (Bar-Matthews et al., 2003). Following MIS 7, the abundance of siderite increases compared to other glacial stages (Fig. 3), indicating that MIS 6 may contain an exceptional climate state that facilitates the generation of siderite.

6.4.5 MIS 5 (130–71 ka)

MIS 5 represents an important interval as it contains the Last Interglacial (MIS 5e), which has been characterised as one of the strongest interglacial periods of the last 800 ka (Lisiecki and Raymo, 2005; Jouzel et al., 2007; Lang and Wolff, 2011). The stage is of interest as enhanced Northern Hemisphere insolation (Berger and Loutre, 1991) and reduced global ice volume (Kopp et al., 2009) provide a measure of climate

BGD
12, 13427–13481, 2015

variability during a time of minimal anthropogenic influence that can potentially be used a partial analogue for present warming and future scenarios, although other MIS may provide a more comprehensive comparison (Loutre and Berger, 2003; Tzedakis et al., 2009b). The record from Lake Ohrid shows the highest average $\delta^{18}O_{lw}$ of the whole sequence during MIS 5 (Fig. 7) and is defined by three clear phases of lower $\delta^{18}O_{lw}$ at approximately ca. 128–112, 107–89, 85–80 ka (thought to roughly correspond to MIS sub-stages 5e, 5c and 5a, respectively), which are punctuated by sub-orbital millennial-scale variations (Fig. 8). The three phases of lower $\delta^{18}O_{lw}$ are broadly comparable with minima in speleothem $\delta^{18}O$ from Israel (Bar-Matthews et al., 2003), which are suggested to represent a distinct increase in regional precipitation due to cyclogenesis and convective activity over the Mediterranean basin (Tzedakis, 2007; Rohling et al., 2015). The enhanced rainfall is coincident with sapropel formation in the eastern Mediterranean (S5, S4, S3, with midpoint ages of 125, 102 and 81 ka, respectively; Ziegler et al., 2010) and high reconstructed sea surface temperatures in the Adriatic Sea (Piva et al., 2008), both of which are a function of precession minima and summer insolation maxima leading to the intensification of summer aridity and greater autumn-winter precipitation (Tzedakis, 2007), which is consistent with higher P/E at Lake Ohrid.

The first phase of low $\delta^{18}O_{lw}$ (ca. 128–112 ka) shows decreasing values from ca. 128 ka to reach a minimum between ca. 124–121 ka, and suggests, combined with exceptionally high TIC (> 8 %), that this period was warm and humid with a high P/E ratio. The decrease is interrupted by a reversal to higher $\delta^{18}O_{lw}$ around ca. 126 ka that indicates reduced P/E and a short-term change to more arid conditions, which is similarly expressed in $\delta^{18}O$ and pollen from the Ioannina basin (Frogley, 1999), Italian speleothem $\delta^{18}O$ (Drysdale et al., 2009; Regattieri et al., 2014), and in Alboran sea surface temperature reconstructions (Martrat et al., 2004). Following a second excursion to higher $\delta^{18}O_{lw}$ at ca. 120 ka, values remain relatively low throughout the remainder of MIS 5e and full interglacial conditions most likely lasted approximately ca. 16 ka, based on the age model for the Ohrid record (Francke et al., 2015), which is in broad agreement with pollen records from the Tenaghi Philippon basin (Tzedakis et al., 2003a) and also Lago Grande di Monticchio (Brauer et al., 2007). A change to higher $\delta^{18}O_{lw}$ is seen between ca. 112–107 ka that probably corresponds to reduced P/E and colder arid climate conditions during stadial phase MIS 5d (Fig. 8). After ca. 107 ka $\delta^{18}O_{lw}$ decreases over the next 4 ka suggesting greater P/E, before beginning a step-wise increase through to ca. 89 ka during MIS 5c that contains several phases of elevated $\delta^{18}O_{lw}$, indicating more pervasive climate variability when compared to the full interglacial (MIS 5e). Although MIS 5e is considered to be warmer and wetter than subsequent interstadials 5c and 5a (Helmens, 2014) with greater summer insolation (Berger and Loutre, 1991), minimum $\delta^{18}O_{lw}$ at Lake Ohrid occurs during the interval corresponding to MIS 5c. This suggests that MIS 5e may have experienced a greater amount of evaporation and seasonal moisture deficiency that would counteract greater precipitation, either forcing P/E to stay constant or to decrease. The increasing $\delta^{18}O_{lw}$ trend observed through MIS 5c ends abruptly after ca. 89 ka, following which there is a large excursion to higher values during MIS 5b (Fig. 8), suggesting much lower P/E and the onset on glacial-like conditions at Lake Ohrid. The transition to this lower P/E phase is evidently more rapid than for MIS 5b, which shows a gradual decline out of the Last Interglacial period, indicating that MIS 5d probably experienced a more pronounced cooling and larger climate shift. The final sub-stage of MIS 5 is a short-lived interstadial that shows less variability than during both MIS 5e and 5c, and has average $\delta^{18}O_{lw}$ equal to MIS 5c.

7 Conclusions

Here, new stable isotope data from the ICDP SCOPSCO 5045-1 composite profile provides valuable information on hydroclimate variability in the northern Mediterranean through the Middle and Late Pleistocene over the last 640 ka. Modern lakewater data (Leng et al., 2010a) and a high-resolution Holocene calibration dataset (Lacey et al., 2014) show that contemporary lakewater is evaporated and that variations in $\delta^{18}O_{lw}$

BGD
12, 13427–13481, 2015

principally reflect changes in P/E driven by regional water balance. The isotope stratigraphy is restricted, in part, due to the cessation of calcite precipitation during glacial (and some stadial) periods, however discrete bands of siderite are typically present throughout these intervals. The siderite was investigated using SEM and determined to be early diagenetic, therefore, like calcite, it captures $\delta^{18}O_{lw}$ at the time of precipitation and is a function of P/E. The isotope composition of both calcite and siderite was converted to $\delta^{18}O_{lw}$ using palaeotemperature equations to enable comparison between the carbonate minerals as they have different equilibrium fractionations and formation temperatures. The modelled $\delta^{18}O_{lw}$ is lower during glacial periods indicating lakewater was fresher than during interglacials most probably due to a combination of cooler summer temperatures and lower evaporation rates, a higher proportion of winter precipitation falling as isotopically light snow, and a reduced inflow from evaporated Lake Prespa. Overall, the isotope data show less evaporative and more stable conditions in MIS 15–13, similar glacial–interglacial $\delta^{18}O_{lw}$ around MIS 9 and MIS 8, and a transition to more evaporated lakewater after MIS 7. The pattern of variability observed in the Lake Ohrid sequence reflects comparable changes in both regional and global palaeoclimate records, and our data highlights the potential for future work on the 5045-1 composite profile to provide evidence for long-term climate change in the Mediterranean, as a prerequisite for better understanding the influence of major environmental events on biological evolution within the lake.

Acknowledgements. Isotope analysis was conducted at the NERC Isotope Geosciences Facility and forms part of the PhD research of JHL funded by the British Geological Survey University Funding Initiative (BUFI). Thanks go to the staff at BGS who assisted with preparation and analysis of isotope samples, in particular Jonathan Dean and Christopher Kendrick, and to John Fletcher of the BGS Thin Sectioning Lab who prepared the thin sections. The SCOPSCO Lake Ohrid drilling campaign was funded by ICDP, the German Ministry of Higher Education and Research, the German Research Foundation, the University of Cologne, the British Geological Survey, the INGV and CNR (both Italy), and the governments of the republics of Macedonia (FYROM) and Albania. Logistic support was provided by the Hydrobiological Institute in Ohrid. Drilling was carried out by Drilling, Observation and Sampling of the Earth's Continental Crust's

(DOSECC) and using the Deep Lake Drilling System (DLDS). Special thanks are due to Beau Marshall and the drilling team. Ali Skinner and Martin Melles provided immense help and advice during logistic preparation and the drilling operation.

References

Albrecht, C. and Wilke, T.: Ancient Lake Ohrid: biodiversity and evolution, Hydrobiologia, 615, 103–140, 2008.

Amataj, S., Anovski, T., Benischke, R., Eftimi, R., Gourcy, L. L., Kola, L., Leontiadis, I., Micevski, E., Stamos, A., and Zoto, J.: Tracer methods used to verify the hypothesis of Cvijić about the underground connection between Prespa and Ohrid Lake, Environ. Geol., 51, 749–753, 2007.

Andrews, J. E., Riding, R., and Dennis, P. F.: Stable isotopic compositions of recent freshwater cyanobacterial carbonates from the British Isles: local and regional environmental controls, Sedimentology, 40, 303–314, 1993.

Anovski, T.: Progress in the Study of Prespa Lake Using Nuclear and Related Techniques, IAEA Regional Project RER/8/008, Skopje, Macedonia, 2001.

Anovski, T., Andonovski, B., and Minceva, B.: HYPERLINK Study of the hydrological relationship between Lakes Ohrid and Prespa, in: Isotope techniques in water resources development: proceedings of an International Symposium on Isotope Techniques in Water Resources Development, IEAE-SM-319/62, IAEA, Vienna, 737–740, 1991.

Anovski, T., Leontiadis, I., and Zoto, J.: Isotope Data, in: Progress in the Study of Prespa Lake Using Nuclear and Related Techniques, edited by: Anovski, T., IAEA Regional Project RER/8/008, 47–52, Faculty of Technology and Metallurgy, The “Ss. Cyril and Methodius” University, Skopje, Republic of Macedonia, 2001.

Anovski, T., Naumovski, J., Kacurkov, D., and Kirkov, P.: A study of the origin of waters of St. Naum Springs, Lake Ohrid, Fizika, 12, 77–86, 1980.

Antonioli, F., Bard, E., Potter, E.-K., Silenzi, S., and Improta, S.: 215 ka history of sea-level oscillations from marine and continental layers in Argentarola Cave speleothems (Italy), Global Planet. Change, 43, 57–78, 2004.

Bahrig, B.: Palaeo-environment information from deep water siderite (Lake of Laach, West Germany), Geological Society, London, Special Publications, 40, 153–158, 1988.

BGD
12, 13427–13481, 2015
Mediterranean climate since the Middle Pleistocene
J. H. Lacey et al.

Balistrieri, L. S., Murray, J. W., and Paul, B.: The cycling of iron and manganese in the water column of Lake Sammamish, Washington, Limnol. Oceanogr., 37, 510–528, 1992.
Bar-Matthews, M., Ayalon, A., and Kaufman, A.: Late quaternary paleoclimate in the Eastern Mediterranean region from stable isotope analysis of speleothems at Soreq Cave, Israel, Quaternary Res., 47, 155–168, 1997.
Bar-Matthews, M., Ayalon, A., Kaufman, A., and Wasserburg, G. J.: The Eastern Mediterranean paleoclimate as a reflection of regional events: Soreq cave, Israel, Earth Planet. Sc. Lett., 166, 85–95, 1999.
Bar-Matthews, M., Ayalon, A., Gilmour, M., Matthews, A., and Hawkesworth, C. J.: Sea-land oxygen isotopic relationships from planktonic foraminifera and speleothems in the Eastern Mediterranean region and their implication for paleorainfall during interglacial intervals, Geochim. Cosmochim. Ac., 67, 3181–3199, 2003.
Bassinot, F. C., Labeyrie, L. D., Vincent, E., Quidelleur, X., Shackleton, N. J., and Lancelot, Y.: The astronomical theory of climate and the age of the Brunhes-Matuyama magnetic reversal, Earth Planet. Sc. Lett., 126, 91–108, 1994.
Baumgarten, H., Wonik, T., Tanner, D. C., Francke, A., Wagner, B., Zanchetta, G., Sulpizio, R., Giaccio, B., and Nomade, S.: Age depth-model for the past 630 ka in Lake Ohrid (Macedonia/Albania) based on cyclostratigraphic analysis of downhole gamma ray data, Biogeosciences Discuss., 12, 7671–7703, doi:10.5194/bgd-12-7671-2015, 2015.
Becker, R. H. and Clayton, R. N.: Oxygen isotope study of a Precambrian banded ironformation, hamersley range, Western Australia, Geochim. Cosmochim. Ac., 40, 1153–1165, 1976.
Belmecheri, S., Namiotko, T., Robert, C., von Grafenstein, U., and Danielopol, D. L.: Climate controlled ostracod preservation in Lake Ohrid (Albania, Macedonia), Palaeogeogr. Palaeocl., 277, 236–245, 2009.
Belmecheri, S., von Grafenstein, U., Andersen, N., Eymard-Bordon, A., Régnier, D., Grenier, C., and Lézine, A.-M.: Ostracod-based isotope record from Lake Ohrid (Balkan Peninsula) over the last 140 ka, Quaternary Sci. Rev., 29, 3894–3904, 2010.
Berger, A. and Loutre, M. F.: Insolation values for the climate of the last 10 million years, Quaternary Sci. Rev., 10, 297–317, 1991.
Bordon, A., Peyron, O., Lézine, A.-M., Brewer, S., and Fouache, E.: Pollen-inferred Late-Glacial and Holocene climate in southern Balkans (Lake Maliq), Quatern. Int., 200, 19–30, 2009.

BGD
12, 13427–13481, 2015

Mediterranean climate since the Middle Pleistocene

J. H. Lacey et al.

Bowen, G. J.: The Online Isotopes in Precipitation Calculator, available at: http://www.waterisotopes.org last access: 18 May 2015.

Bowen, G. J., Wassenaar, L. I., and Hobson, K. A.: Global application of stable hydrogen and oxygen isotopes to wildlife forensics, Oecologia, 143, 337–348, 2005.

Brauer, A., Allen, J. R., Mingram, J., Dulski, P., Wulf, S., and Huntley, B.: Evidence for last interglacial chronology and environmental change from Southern Europe, P. Natl. Acad. Sci. USA, 104, 450–455, 2007.

Brauer, A. and Negendank, J. F. W.: Paleoenvironmental reconstruction of the Late- and Postglacial sedimentary record of Lake Weinfelder Maar, in: Paleolimnology of European Maar Lakes, edited by: Negendank, J. W., and Zolitschka, B., Lecture Notes in Earth Sciences, Springer, Berlin, Heidelberg, 1993.

Carothers, W. W., Adami, L. H., and Rosenbauer, R. J.: Experimental oxygen isotope fractionation between siderite-water and phosphoric acid liberated CO_2-siderite, Geochim. Cosmochim. Ac., 52, 2445–2450, 1988.

Chukanov, N. V.: Infrared Spectra of Mineral Species, Springer , Dordrecht, Heidelberg, New York, London, 2014.

Cohen, A. S.: Paleolimnology: The History and Evolution of Lake Systems, Oxford University Press, Oxford, 2003.

Coleman, M. L.: Geochemistry of diagenetic non-silicate minerals: kinetic considerations, Philos. T. R. Soc. Lond.-A, 315, 39–56, 1985.

Craig, H.: Isotopic variations in meteoric waters, Science, 133, 1702–1703, 1961.

Craig, H.: The measurement of oxygen isotope palaeotemperatures, in: Stable Isotopes in Oceanographic Studies and Palaeotemperatures, edited by: Tongiorgi, E., Consiglio Nazionale delle Ricerche Laboratorio di Geologia Nucleare, Pisa, 1965.

Curry, B. B., Anderson, T. F., and Lohmann, K. C.: Unusual carbon and oxygen isotopic ratios of ostracodal calcite from last interglacial (Sangamon episode) lacustrine sediment in Raymond Basin, Illinois, USA, J. Paleolimnol., 17, 421–435, 1997.

Dansgaard, W.: Stable isotopes in precipitation, Tellus, 16, 436–468, 1964.

Darling, W. G., Bath, A. H., Gibson, J. J., and Rozanski, K.: Isotopes in Palaeoenvironmental Research: 1. Isotopes in Water, Springer, Netherlands, 2006.

Dean, J. R., Jones, M. D., Leng, M. J., Sloane, H. J., Roberts, C. N., Woodbridge, J., Swann, G. E. A., Metcalfe, S. E., Eastwood, W. J., and Yiğitbaşıoğlu, H.: Palaeo-seasonality

of the last two millennia reconstructed from the oxygen isotope composition of carbonates and diatom silica from Nar Gölü, central Turkey, Quaternary Sci. Rev., 66, 35–44, 2013.
Drysdale, R. N., Hellstrom, J. C., Zanchetta, G., Fallick, A. E., Sánchez Goñi, M. F., Couchoud, I., McDonald, J., Maas, R., Lohmann, G., and Isola, I.: Evidence for obliquity forcing of glacial termination II, Science, 325, 1527–1531, 2009.
Eastwood, W. J., Leng, M. J., Roberts, N., and Davis, B.: Holocene climate change in the eastern Mediterranean region: a comparison of stable isotope and pollen data from Lake Gölhisar, southwest Turkey, J. Quaternary Sci., 22, 327–341, 2007.
Eftimi, R. and Zoto, J.: Isotope study of the connection of Ohrid and Prespa lakes. International Symposium "Towards Integrated Conservation and Sustainable Development of Transboundary Macro and Micro Prespa Lakes", 32–37, Korcha, Albania, 24–26 October 1997.
Eftimi, R., Micevski, E., and Stamos, A.: Geological and hydrogeological conditions of the Prespa Region. in: Progress in the Study of Prespa Lake Using Nuclear and Related Techniques, edited by: Anovski, T., IAEA Regional Project RER/8/008, 11–22, Faculty of Technology and Metallurgy, The "Ss. Cyril and Methodius" University, Skopje, Republic of Macedonia, 2001.
Epstein, S., Buchsbaum, R., Lowenstam, H. A., and Urey, H. C.: Revised carbonate-water isotopic temperature scale, Geol. Soc. Am. Bull., 64, 1315–1326, 1953.
Francke, A., Wagner, B., Just, J., Leicher, N., Gromig, R., Baumgarten, H., Vogel, H., Lacey, J. H., Sadori, L., Wonik, T., Leng, M. J., Zanchetta, G., Sulpizio, R., and Giacco, B.: Sedimentological processes and environmental variability at Lake Ohrid (Macedonia, Albania) between 640 ka and present day, Biogeosciences Discuss., in preparation, 2015.
Francke, A., Wagner, B., Leng, M. J., and Rethemeyer, J.: A Late Glacial to Holocene record of environmental change from Lake Dojran (Macedonia, Greece), Clim. Past, 9, 481–498, doi:10.5194/cp-9-481-2013, 2013.
Frogley, M. R.: Climate variability in Northwest Greece during the last interglacial, Science, 285, 1886–1889, 1999.
Frogley, M. R., Griffiths, H. I., and Heaton, T. H. E.: Historical biogeography and Late Quaternary environmental change of Lake Pamvotis, Ioannina (north-western Greece): evidence from ostracods, J. Biogeogr., 28, 745–756, 2001.
García-Ruiz, J. M., López-Moreno, J. I., Vicente-Serrano, S. M., Lasanta-Martínez, T., and Beguería, S.: Mediterranean water resources in a global change scenario, Earth-Sci. Rev., 105, 121–139, 2011.

Giannakopoulos, C., Le Sager, P., Bindi, M., Moriondo, M., Kostopoulou, E., and Goodess, C. M.: Climatic changes and associated impacts in the Mediterranean resulting from a 2 °C global warming, Global Planet. Change, 68, 209–224, 2009.
Giorgi, F.: Climate change hot-spots, Geophys. Res. Lett., 33, L08707, doi:10.1029/2006GL025734, 2006.
Granina, L., Müller, B., and Wehrli, B.: Origin and dynamics of Fe and Mn sedimentary layers in Lake Baikal, Chem. Geol., 205, 55–72, 2004.
Hadzisce, S.: Das Mixophänomen im Ohridsee im Laufe der Jahre 1941/42–1964/65, Verhandlungen des Internationalen Verein Limnologie, 16, 134–138, 1966.
Hammarlund, D., Aravena, R., Barnekow, L., Buchardt, B., and Possnert, G.: Multi-component carbon isotope evidence of early Holocene environmental change and carbon-flow pathways from a hard-water lake in northern Sweden, J. Paleolimnol., 18, 219–233, 1997.
Helmens, K. F.: The Last Interglacial–Glacial cycle (MIS 5-2) re-examined based on long proxy records from central and northern Europe, Quaternary Sci. Rev., 86, 115–143, 2014.
Hoefs, J.: Stable Isotope Geochemistry, Springer-Verlag, Berlin, 1980.
Hollis, G. E. and Stevenson, A. C.: The physical basis of the Lake Mikri Prespa systems: geology, climate, hydrology and water quality, Hydrobiologia, 351, 1–19, 1997.
Hudson, J. D.: Stable isotopes and limestone lithification, J. Geol. Soc. London, 133, 637–660, 1977.
Imbrie, J., Hays, J. D., Martinson, D. G., McIntyre, A., Mix, A. C., Morley, J. J., Pisias, N. G., Prell, W. L., and Shackleton, N.: The orbital theory of Pleistocene climate: support from a revised chronology of the marine δ18O record. in: Milankovitch and Climate (Part 1), edited by: Berger, A., Imbrie, J., Hays, H., Kukla, G., and Saltzman, B., Reidel, Hingham, Mass., 1984.
Jin, L., Ogrinc, N., Hamilton, S. K., Szramek, K., Kanduc, T., and Walter, L. M.: Inorganic carbon isotope systematics in soil profiles undergoing silicate and carbonate weathering (Southern Michigan, USA), Chem. Geol., 264, 139–153, 2009.
Jones, M. D., Roberts, C. N., and Leng, M. J.: Quantifying climatic change through the last glacial–interglacial transition based on lake isotope palaeohydrology from central Turkey, Quaternary Res., 67, 463–473, 2007.
Jordanoska, B., Kunz, M. J., Stafilov, T., and Wuest, A.: Temporal variability in physico-chemical properties of St. Naum karst springs feeding Lake Ohrid, Ecology and Protection of the Environment, 13, 3–11, 2010.

BGD
12, 13427–13481, 2015

Mediterranean climate since the Middle Pleistocene

J. H. Lacey et al.

Jouzel, J., Masson-Delmotte, V., Cattani, O., Dreyfus, G., Falourd, S., Hoffmann, G., Minster, B., Nouet, J., Barnola, J. M., Chappellaz, J., Fischer, H., Gallet, J. C., Johnsen, S., Leuenberger, M., Loulergue, L., Luethi, D., Oerter, H., Parrenin, F., Raisbeck, G., Raynaud, D., Schilt, A., Schwander, J., Selmo, E., Souchez, R., Spahni, R., Stauffer, B., Steffensen, J. P., Stenni, B., Stocker, T. F., Tison, J. L., Werner, M., and Wolff, E. W.: Orbital and millennial antarctic climate variability over the past 800,000 years, Science, 317, 793–796, 2007.

Katsuta, N., Takano, M., Kawakami, S.-I., Togami, S., Fukusawa, H., Kumazawa, M., and Yasuda, Y.: Climate system transition from glacial to interglacial state around the beginning of the last termination: evidence from a centennial- to millennial-scale climate rhythm, Geochem. Geophy. Geosy., 7, Q12006, doi:10.1029/2006GC001310, 2006.

Kim, S. T. and ONeil, J. R.: Equilibrium and nonequilibrium oxygen isotope effects in synthetic carbonates, Geochim. Cosmochim. Ac., 61, 3461–3475, 1997.

Kopp, R. E., Simons, F. J., Mitrovica, J. X., Maloof, A. C., and Oppenheimer, M.: Probabilistic assessment of sea level during the last interglacial stage, Nature, 462, 863–867, 2009.

Kroon, D., Alexander, I., Little, M., Lourens, L. J., Mattewson, A., Robertson, A. H. F., and Sakamoto, T.: 14. Oxygen isotope and sapropel stratigraphy in the eastern Mediterranean during the last 3.2 million years. in: Proceedings of the Ocean Drilling Program, edited by: Robertson, A. H. F., Emeis, K.-C., Richter, C., and Camerlenghi, A., Scientific Results, Vol. 160, 181–189, Ocean Drilling Program, 1998.

Krylov, A., Khlystov, O., Zemskaya, T., Minami, H., Hachikubo, A., Nunokawa, Y., Kida, M., Shoji, H., Naudts, L., Poort, J., and Pogodaeva, T.: First discovery and formation process of authigenic siderite from gas hydrate–bearing mud volcanoes in fresh water: Lake Baikal, eastern Siberia, Geophys. Res. Lett., 35, L05405, doi:10.1029/2007GL032917, 2008.

Kwiecien, O., Stockhecke, M., Pickarski, N., Heumann, G., Litt, T., Sturm, M., Anselmetti, F., Kipfer, R., and Haug, G. H.: Dynamics of the last four glacial terminations recorded in Lake Van, Turkey, Quaternary Sci. Rev., 104, 42–52, 2014.

Lacey, J. H., Francke, A., Leng, M. J., Vane, C. H., and Wagner, B.: A high-resolution Late Glacial to Holocene record of environmental change in the Mediterranean from Lake Ohrid (Macedonia/Albania), Int. J. Earth Sci., doi:10.1007/s00531-014-1033-6, 2014.

Lang, N. and Wolff, E. W.: Interglacial and glacial variability from the last 800 ka in marine, ice and terrestrial archives, Clim. Past, 7, 361–380, doi:10.5194/cp-7-361-2011, 2011.

BGD
12, 13427–13481, 2015

Laskar, J., Robutel, P., Joutel, F., Gastineau, M., Correia, A. C. M., and Levrard, B.: A long-term numerical solution for the insolation quantities of the Earth, Astron. Astrophys., 428, 261–285, 2004.
Lebeau, O., Busigny, V., Chaduteau, C., and Ader, M.: Organic matter removal for the analysis of carbon and oxygen isotope compositions of siderite, Chem. Geol., 372, 54–61, 2014.
Leicher, N., Zanchetta, G., Sulpizio, R., Giaccio, B., Wagner, B., Nomade, S., and Francke, A.: First tephrostratigraphic results of the DEEP site record in Lake Ohrid, Macedonia, Biogeosciences Discuss., in preparation, 2015.
Leng, M. J. and Marshall, J. D.: Palaeoclimate interpretation of stable isotope data from lake sediment archives, Quaternary Sci. Rev., 23, 811–831, 2004.
Leng, M. J., Baneschi, I., Zanchetta, G., Jex, C. N., Wagner, B., and Vogel, H.: Late Quaternary palaeoenvironmental reconstruction from Lakes Ohrid and Prespa (Macedonia/Albania border) using stable isotopes, Biogeosciences, 7, 3109–3122, doi:10.5194/bg-7-3109-2010, 2010a.
Leng, M. J., Jones, M. D., Frogley, M. R., Eastwood, W. J., Kendrick, C. P., and Roberts, C. N.: Detrital carbonate influences on bulk oxygen and carbon isotope composition of lacustrine sediments from the Mediterranean, Global Planet. Change, 71, 175–182, 2010b.
Leng, M. J., Wagner, B., Boehm, A., Panagiotopoulos, K., Vane, C. H., Snelling, A., Haidon, C., Woodley, E., Vogel, H., Zanchetta, G., and Baneschi, I.: Understanding past climatic and hydrological variability in the Mediterranean from Lake Prespa sediment isotope and geochemical record over the Last Glacial cycle, Quaternary Sci. Rev., 66, 123–136, 2013.
Lézine, A. M., von Grafenstein, U., Andersen, N., Belmecheri, S., Bordon, A., Caron, B., Cazet, J. P., Erlenkeuser, H., Fouache, E., Grenier, C., Huntsman-Mapila, P., Hureau-Mazaudier, D., Manelli, D., Mazaud, A., Robert, C., Sulpizio, R., Tiercelin, J. J., Zanchetta, G., and Zeqollari, Z.: Lake Ohrid, Albania, provides an exceptional multi-proxy record of environmental changes during the last glacial–interglacial cycle, Palaeogeogr. Palaeocl., 287, 116–127, 2010.
Li, H. C. and Ku, T. L.: δ13C-δ18O covariance as a paleohydrological indicator for closed-basin lakes, Palaeogeogr. Palaeocl., 133, 69–80, 1997.
Linacre, E.: Climate Data and Resources: A Reference and Guide, Routledge, London, 1992.
Lindhorst, K., Vogel, H., Krastel, S., Wagner, B., Hilgers, A., Zander, A., Schwenk, T., Wessels, M., and Daut, G.: Stratigraphic analysis of lake level fluctuations in Lake Ohrid: an

integration of high resolution hydro-acoustic data and sediment cores, Biogeosciences, 7, 3531–3548, doi:10.5194/bg-7-3531-2010, 2010.
Lindhorst, K., Krastel, S., Reicherter, K., Stipp, M., Wagner, B., and Schwenk, T.: Sedimentary and tectonic evolution of Lake Ohrid (Macedonia/Albania), Basin Res., 27, 84–101, 2015.
Lisiecki, L. E. and Raymo, M. E.: A Pliocene-Pleistocene stack of 57 globally distributed benthic δ18O records, Paleoceanography, 20, PA1003, doi:10.1029/2004PA001071, 2005.
Litt, T., Pickarski, N., Heumann, G., Stockhecke, M., and Tzedakis, P. C.: A 600,000 year long continental pollen record from Lake Van, eastern Anatolia (Turkey), Quaternary Sci. Rev., 104, 30–41, 2014.
Loulergue, L., Schilt, A., Spahni, R., Masson-Delmotte, V., Blunier, T., Lemieux, B., Barnola, J. M., Raynaud, D., Stocker, T. F., and Chappellaz, J.: Orbital and millennial-scale features of atmospheric CH_4 over the past 800,000 years, Nature, 453, 383–386, 2008.
Loutre, M. F. and Berger, A.: Marine isotope stage 11 as an analogue for the present interglacial, Global Planet. Change, 36, 209–217, 2003.
Ludvigson, G. A., González, L. A., Fowle, D. A., Roberts, J. A., Driese, S. G., Villarreal, M. A., Smith, J. J., and Suarez, M. B.: Paleoclimatic Applications and Modern Process Studies of Pedogenic Siderite, in: New Frontiers in Paleopedology and Terrestrial Paleoclimatology, SEPM (Society for Sedimentary Geology) Special Publication, edited by: Driese, S. G. and Nordt, L. C., 104, 79–87, 2013.
Lüthi, D., Le Floch, M., Bereiter, B., Blunier, T., Barnola, J. M., Siegenthaler, U., Raynaud, D., Jouzel, J., Fischer, H., Kawamura, K., and Stocker, T. F.: High-resolution carbon dioxide concentration record 650,000–800,000 years before present, Nature, 453, 379–382, 2008.
Magny, M., Combourieu-Nebout, N., de Beaulieu, J. L., Bout-Roumazeilles, V., Colombaroli, D., Desprat, S., Francke, A., Joannin, S., Ortu, E., Peyron, O., Revel, M., Sadori, L., Siani, G., Sicre, M. A., Samartin, S., Simonneau, A., Tinner, W., Vannière, B., Wagner, B., Zanchetta, G., Anselmetti, F., Brugiapaglia, E., Chapron, E., Debret, M., Desmet, M., Didier, J., Essallami, L., Galop, D., Gilli, A., Haas, J. N., Kallel, N., Millet, L., Stock, A., Turon, J. L., and Wirth, S.: North–south palaeohydrological contrasts in the central Mediterranean during the Holocene: tentative synthesis and working hypotheses, Clim. Past, 9, 2043–2071, doi:10.5194/cp-9-2043-2013, 2013.
Maiorano, P., Tarantino, F., Marino, M., and De Lange, G. J.: Paleoenvironmental conditions at core KC01B (Ionian Sea) through MIS 13-9: evidence from calcareous nannofossil assemblages, Quatern. Int., 288, 97–111, 2013.

Martrat, B., Grimalt, J. O., Lopez-Martinez, C., Cacho, I., Sierro, F. J., Flores, J. A., Zahn, R., Canals, M., Curtis, J. H., and Hodell, D. A.: Abrupt temperature changes in the Western Mediterranean over the past 250,000 years, Science, 306, 1762–1765, 2004.

Martrat, B., Grimalt, J. O., Shackleton, N. J., De Abreu, L., Hutterli, M. A., and Stocker, T. F.: Four climate cycles of recurring deep and surface water destabilizations on the Iberian Margin, Science, 27, 502–507, 2007.

Masson-Delmotte, V., Stenni, B., Pol, K., Braconnot, P., Cattani, O., Falourd, S., Kageyama, M., Jouzel, J., Landais, A., Minster, B., Barnola, J. M., Chappellaz, J., Krinner, G., Johnsen, S., Röthlisberger, R., Hansen, J., Mikolajewicz, U., and Otto-Bliesner, B.: EPICA Dome C record of glacial and interglacial intensities, Quaternary Sci. Rev., 29, 113–128, 2010.

Matter, M., Anselmetti, F. S., Jordanoska, B., Wagner, B., Wessels, M., and Wüest, A.: Carbonate sedimentation and effects of eutrophication observed at the Kališta subaquatic springs in Lake Ohrid (Macedonia), Biogeosciences, 7, 3755–3767, doi:10.5194/bg-7-3755-2010, 2010.

Matzinger, A., Jordanoski, M., Veljanoska-Sarafiloska, E., Sturm, M., Müller, B., and Wüest, A.: Is Lake Prespa jeopardizing the ecosystem of ancient Lake Ohrid?, Hydrobiologia, 553, 89–109, 2006a.

Matzinger, A., Spirkovski, Z., Patceva, S., and Wüest, A.: Sensitivity of ancient Lake Ohrid to local anthropogenic impacts and global warming, J. Great Lakes Res., 32, 158–179, 2006b.

Matzinger, A., Schmid, M., Veljanoska-Sarafiloska, E., Patceva, S., Guseska, D., Wagner, B., Müller, B., Sturm, M., and Wüest, A.: Eutrophication of ancient Lake Ohrid: global warming amplifies detrimental effects of increased nutrient inputs, Limnol. Oceanogr., 52, 338–353, 2007.

McKenzie, J. A.: Carbon isotopes and productivity in the lacustrine and marine environment. in: Chemical Processes in Lakes, edited by: Stumm, W., Wiley, New York, 99–118, 1985.

McManus, J. F.: A 0.5-million-year record of millennial-scale climate variability in the North Atlantic, Science, 283, 971–975, 1999.

Meyers, P. A. and Teranes, J. L.: Sediment Organic Matter. in: Tracking Environmental Change Using Lake Sediments, edited by: Last, W. M., and Smol, J. P., Developments in Paleoenvironmental Research, Springer, the Netherlands, 2001.

Mozley, P. S. and Wersin, P.: Isotopic composition of siderite as an indicator of depositional environment, Geology, 20, 817–820, 1992.

BGD
12, 13427–13481, 2015
Mediterranean climate since the Middle Pleistocene
J. H. Lacey et al.

O'Neil, J. R., Clayton, R. N., and Mayeda, T. K.: Oxygen Isotope Fractionation in Divalent Metal Carbonates, J. Chem. Phys., 51, 5547–5558, 1969.

Panagiotopoulos, K., Aufgebauer, A., Schäbitz, F., and Wagner, B.: Vegetation and climate history of the Lake Prespa region since the Lateglacial, Quatern. Int., 293, 157–169, 2013.

Panagiotopoulos, K., Böhm, A., Leng, M. J., Wagner, B., and Schäbitz, F.: Climate variability over the last 92 ka in SW Balkans from analysis of sediments from Lake Prespa, Clim. Past, 10, 643–660, doi:10.5194/cp-10-643-2014, 2014.

Patceva S. and Mitic V.: A comparison of vertical and seasonal distribution of chlorophyll *a* in Lakes Ohrid and Prespa, BALWOIS 2008-374, Ohrid, Republic of Macedonia, 27–31 May, 1–8, http://balwois.com/wp-content/uploads/old_proc/ffp-1255.pdf (last access: 21 April 2015), 2008.

Petit, J. R., Jouzel, J., Raynaud, D., Barkov, N. I., Barnola, J. M., Basile, I., Bender, M., Chappellaz, J., Davis, M., Delaygue, G., Delmotte, M., Kotlyakov, V. M., Legrand, M., Lipenkov, V. Y., Lorius, C., Pepin, L., Ritz, C., Saltzman, E., and Stievenard, M.: Climate and atmospheric history of the past 420,000 years from the Vostok ice core, Antarctica, Nature, 399, 429–436, 1999.

Piva, A., Asioli, A., Andersen, N., Grimalt, J. O., Schneider, R. R., and Trincardi, F.: Climatic cycles as expressed in sediments of the PROMESS1 borehole PRAD1-2, central Adriatic, for the last 370 ka: 2. Paleoenvironmental evolution, Geochem. Geophy. Geosy., 9, Q03R02, doi:10.1029/2007GC001785, 2008.

Popovska, C. and Bonacci, O.: Basic data on the hydrology of Lakes Ohrid and Prespa, Hydrol. Process., 21, 658–664, 2007.

Prokopenko, A. A., Hinnov, L. A., Williams, D. F., and Kuzmin, M. I.: Orbital forcing of continental climate during the Pleistocene: a complete astronomically tuned climatic record from Lake Baikal, SE Siberia, Quaternary Sci. Rev., 25, 3431–3457, 2006.

Prokopenko, A. A., Williams, D. F., Kuzmin, M. I., Karabanov, E. B., Khursevich, G. K., and Peck, J. A.: Muted climate variations in continental Siberia during the mid-Pleistocene epoch, Nature, 418, 65–68, 2002.

Railsback, L. B., Gibbard, P. L., Head, M. J., Voarintsoa, N. R. G., and Toucanne, S.: An optimized scheme of lettered marine isotope substages for the last 1.0 million years, and the climatostratigraphic nature of isotope stages and substages, Quaternary Sci. Rev., 111, 94–106, 2015.

Regattieri, E., Zanchetta, G., Drysdale, R. N., Isola, I., Hellstrom, J. C., and Roncioni, A.: A continuous stable isotope record from the penultimate glacial maximum to the Last Interglacial (159–121ka) from Tana Che Urla Cave (Apuan Alps, central Italy), Quaternary Res., 82, 450–461, 2014.

Regattieri, E., Giaccio, B., Zanchetta, G., Drysdale, R. N., Galli, P., Nomade, S., Peronace, E., and Wulf, S.: Hydrological variability over the Apennines during the early last glacial precession minimum, as revealed by a stable isotope record from Sulmona basin, Central Italy, J. Quaternary Sci., 30, 19–31, 2015.

Roberts, N., Reed, J. M., Leng, M. J., Kuzucuoglu, C., Fontugne, M., Bertaux, J., Woldring, H., Bottema, S., Black, S., Hunt, E., and Karabiyikoglu, M.: The tempo of Holocene climatic change in the eastern Mediterranean region: New high-resolution crater-lake sediment data from central Turkey, Holocene, 11, 721–736, 2001.

Roberts, N., Jones, M. D., Benkaddour, A., Eastwood, W. J., Filippi, M. L., Frogley, M. R., Lamb, H. F., Leng, M. J., Reed, J. M., Stein, M., Stevens, L., Valero-Garcés, B., and Zanchetta, G.: Stable isotope records of Late Quaternary climate and hydrology from Mediterranean lakes: the ISOMED synthesis, Quaternary Sci. Rev., 27, 2426–2441, 2008.

Rodrigues, T., Voelker, A. H. L., Grimalt, J. O., Abrantes, F., and Naughton, F.: Iberian Margin sea surface temperature during MIS 15 to 9 (580–300 ka): glacial suborbital variability vs. interglacial stability, Paleoceanography, 26, PA1204, doi:10.1029/2010PA001927, 2011.

Rohling, E. J., Marino, G., and Grant, K. M.: Mediterranean climate and oceanography, and the periodic development of anoxic events (sapropels), Earth-Sci. Rev., 143, 62–97, 2015.

Rosenbaum, J. and Sheppard, S. M. F.: An isotopic study of siderites, dolomites and ankerites at high temperatures, Geochim. Cosmochim. Ac., 50, 1147–1150, 1986.

Rossignol-Strick, M. and Paterne, M.: A synthetic pollen record of the eastern Mediterranean sapropels of the last 1 Ma: implications for the time-scale and formation of sapropels, Mar. Geol., 153, 221–237, 1999.

Roucoux, K. H., Tzedakis, P. C., Frogley, M. R., Lawson, I. T., and Preece, R. C.: Vegetation history of the marine isotope stage 7 interglacial complex at Ioannina, NW Greece, Quaternary Sci. Rev., 27, 1378–1395, 2008.

Shackleton, N. J.: The 100,000-year ice-age cycle identified and found to lag temperature, carbon dioxide, and orbital eccentricity, Science, 289, 1897–1902, 2000.

Siani, G., Paterne, M., and Colin, C.: Late glacial to Holocene planktic foraminifera bioevents and climatic record in the South Adriatic Sea, J. Quaternary Sci., 25, 808–821, 2010.

Stankovic, S.: The Balkan Lake Ohrid and Its Living World, Monographiae Biologicae, Volume IX, Dr. W. Junk Publishers, The Hague, the Netherlands, 1–357, 1960.

Stein, R., Hefter, J., Grützner, J., Voelker, A., and Naafs, B. D. A.: Variability of surface water characteristics and Heinrich-like events in the Pleistocene midlatitude North Atlantic Ocean: biomarker and XRD records from IODP Site U1313 (MIS 16–9), Paleoceanography, 24, PA2203, doi:10.1029/2008PA001639, 2009.

Stevens, L. R., Wright Jr., H.E, and Ito, E.: Proposed changes in seasonality of climate during the Lateglacial and Holocene at Lake Zeribar, Iran, Holocene, 11, 747–755, 2001.

Sun, Y. and An, Z.: Late Pliocene-Pleistocene changes in mass accumulation rates of eolian deposits on the central Chinese Loess Plateau, J. Geophys. Res., 110, D23101, doi:10.1029/2005JD006064, 2005.

Talbot, M. R.: A review of the palaeohydrological interpretation of carbon and oxygen isotopic ratios in primary lacustrine carbonates, Chem. Geol.: Isotope Geoscience section, 80, 261–279, 1990.

Torfstein, A., Haase-Schramm, A., Waldmann, N., Kolodny, Y., and Stein, M.: U-series and oxygen isotope chronology of the mid-Pleistocene Lake Amora (Dead Sea basin), Geochim. Cosmochim. Ac., 73, 2603–2630, 2009.

Tzedakis, P. C.: Seven ambiguities in the Mediterranean palaeoenvironmental narrative, Quaternary Sci. Rev., 26, 2042–2066, 2007.

Tzedakis, P. C., Andrieu, V., deBeaulieu, J. L., Crowhurst, S., Follieri, M., Hooghiemstra, H., Magri, D., Reille, M., Sadori, L., Shackleton, N. J., and Wijmstra, T. A.: Comparison of terrestrial and marine records of changing climate of the last 500,000 years, Earth Planet. Sc. Lett., 150, 171–176, 1997.

Tzedakis, P. C., Frogley, M. R., and Heaton, T. H. E.: Last Interglacial conditions in southern Europe: evidence from Ioannina, northwest Greece, Global Planet. Change, 36, 157–170, 2003a.

Tzedakis, P. C., McManus, J. F., Hooghiemstra, H., Oppo, D. W., and Wijmstra, T. A.: Comparison of changes in vegetation in northeast Greece with records of climate variability on orbital and suborbital frequencies over the last 450 000 years, Earth Planet. Sc. Lett., 212, 197–212, 2003b.

Tzedakis, P. C., Hooghiemstra, H., and Pälike, H.: The last 1.35 million years at Tenaghi Philippon: revised chronostratigraphy and long-term vegetation trends, Quaternary Sci. Rev., 25, 3416–3430, 2006.

BGD
12, 13427–13481, 2015
Mediterranean climate since the Middle Pleistocene
J. H. Lacey et al.

Tzedakis, P. C., Pälike, H., Roucoux, K. H., and de Abreu, L.: Atmospheric methane, southern European vegetation and low-mid latitude links on orbital and millennial timescales, Earth Planet. Sc. Lett., 277, 307–317, 2009a.

Tzedakis, P. C., Raynaud, D., McManus, J. F., Berger, A., Brovkin, V., and Kiefer, T.: Interglacial diversity, Nature, 2, 751–755, 2009b.

Usdowski, E. and Hoefs, J.: Kinetic $^{13}C^{12}C$ and $^{18}O^{16}O$ effects upon dissolution and outgassing of CO_2 in the system CO_2H_2O, Chem. Geol.: Isotope Geoscience Section, 80, 109–118, 1990.

Vogel, H., Wagner, B., Zanchetta, G., Sulpizio, R., and Rosén, P.: A paleoclimate record with tephrochronological age control for the last glacial–interglacial cycle from Lake Ohrid, Albania and Macedonia, J. Paleolimnol., 44, 295–310, 2010.

Wagner, B., Reicherter, K., Daut, G., Wessels, M., Matzinger, A., Schwalb, A., Spirkovski, Z., and Sanxhaku, M.: The potential of Lake Ohrid for long-term palaeoenvironmental reconstructions, Palaeogeogr. Palaeocl., 259, 341–356, 2008.

Wagner, B., Lotter, A. F., Nowaczyk, N., Reed, J. M., Schwalb, A., Sulpizio, R., Valsecchi, V., Wessels, M., and Zanchetta, G.: A 40,000 year record of environmental change from ancient Lake Ohrid (Albania and Macedonia), J. Paleolimnol., 41, 407–430, 2009.

Wagner, B., Vogel, H., Zanchetta, G., and Sulpizio, R.: Environmental change within the Balkan region during the past ca. 50 ka recorded in the sediments from lakes Prespa and Ohrid, Biogeosciences, 7, 3187–3198, doi:10.5194/bg-7-3187-2010, 2010.

Wagner, B., Francke, A., Sulpizio, R., Zanchetta, G., Lindhorst, K., Krastel, S., Vogel, H., Rethemeyer, J., Daut, G., Grazhdani, A., Lushaj, B., and Trajanovski, S.: Possible earthquake trigger for 6th century mass wasting deposit at Lake Ohrid (Macedonia/Albania), Clim. Past, 8, 2069–2078, doi:10.5194/cp-8-2069-2012, 2012.

Wagner, B., Wilke, T., Krastel, S., Zanchetta, G., Sulpizio, R., Reicherter, K., Leng, M. J., Grazhdani, A., Trajanovski, S., Francke, A., Lindhorst, K., Levkov, Z., Cvetkoska, A., Reed, J. M., Zhang, X., Lacey, J. H., Wonik, T., Baumgarten, H., and Vogel, H.: The SCOPSCO drilling project recovers more than 1.2 million years of history from Lake Ohrid, Sci. Dril., 17, 19–29, doi:10.5194/sd-17-19-2014, 2014.

Wersin, P., Hohener, P., Giovanoli, R., and Stumm, W.: Early diagenetic influences on iron transformations in a fresh-water lake sediment, Chem. Geol., 90, 233–252, 1991.

White, W. B.: The carbonate minerals. in: The Infrared Spectra of Minerals, edited by: Farmer, V. C., Mineralogical Society Monograph, 4, Adlard and Son, Dorking, Surrey, 227–284, 1974.

Wick, L., Lemcke, G., and Sturm, M.: Evidence of Lateglacial and Holocene climatic change and human impact in eastern Anatolia: high-resolution pollen, charcoal, isotopic and geochemical records from the laminated sediments of Lake Van, Turkey, Holocene, 13, 665–675, 2003.

WMO: World Weather Information Service, Hong Kong Observatory, Hong Kong, 2015.

Yu, P.-S., and Chen, M.-T.: A prolonged warm and humid interval during marine isotope stage 13–15 as revealed by hydrographic reconstructions from the South China Sea (IMAGES MD972142), J. Asian Earth Sci., 40, 1230–1237, 2011.

Zanchetta, G., Borghini, A., Fallick, A. E., Bonadonna, F. P., and Leone, G.: Late Quaternary palaeohydrology of Lake Pergusa (Sicily, southern Italy) as inferred by stable isotopes of lacustrine carbonates, J. Paleolimnol., 38, 227–239, 2007.

Zhang, C. L., Horita, J., Cole, D. R., Zhou, J. Z., Lovley, D. R., and Phelps, T. J.: Temperature-dependent oxygen and carbon isotope fractionations of biogenic siderite, Geochim. Cosmochim. Ac., 65, 2257–2271, 2001.

Ziegler, M., Tuenter, E., and Lourens, L. J.: The precession phase of the boreal summer monsoon as viewed from the eastern Mediterranean (ODP Site 968), Quaternary Sci. Rev., 29, 1481–1490, 2010.

BGD

12, 13427–13481, 2015

Mediterranean climate since the Middle Pleistocene

J. H. Lacey et al.

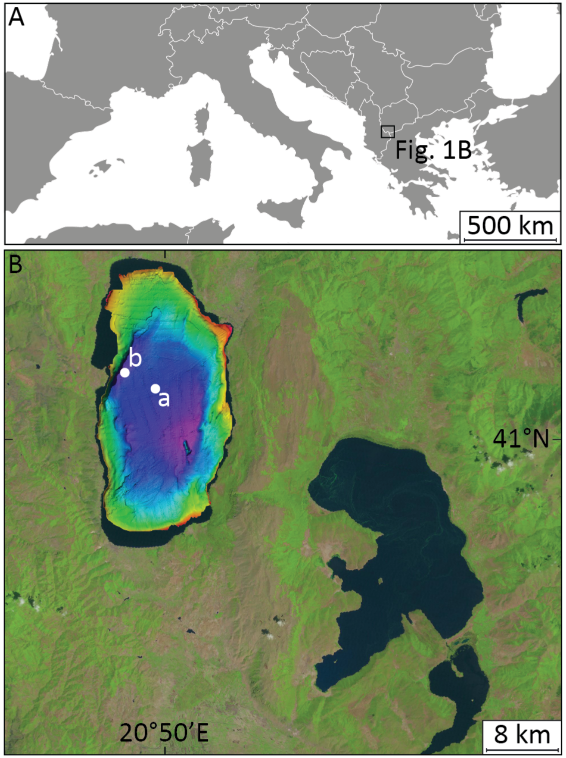

Figure 1. (a) Map of southern Europe and the northern Mediterranean showing the location of **(b)**. **(b)** Landsat map of Lake Ohrid and Lake Prespa indicating the locations of coring sites **(a)** DEEP 5045-1 and **(b)** Lini Co1262 (Wagner et al., 2012; Lacey et al., 2014). Bathymetric map of Lake Ohrid from Lindhorst et al. (2015).

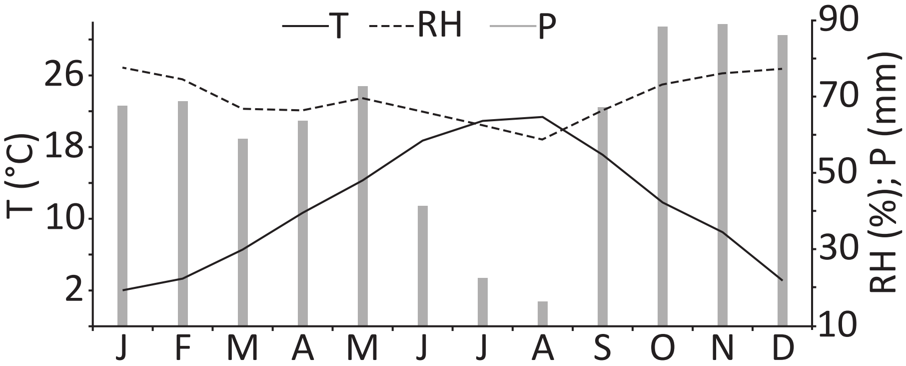

Figure 2. Recent climate data from the town of Ohrid (WMO station 135780; 41.1170° N, 20.8000° E, 761 m a.s.l.) showing monthly averages over the period 2010–2014 for average temperature (T), precipitation (P) and relative humidity (RH) (data available from WMO, 2015).

BGD
12, 13427–13481, 2015

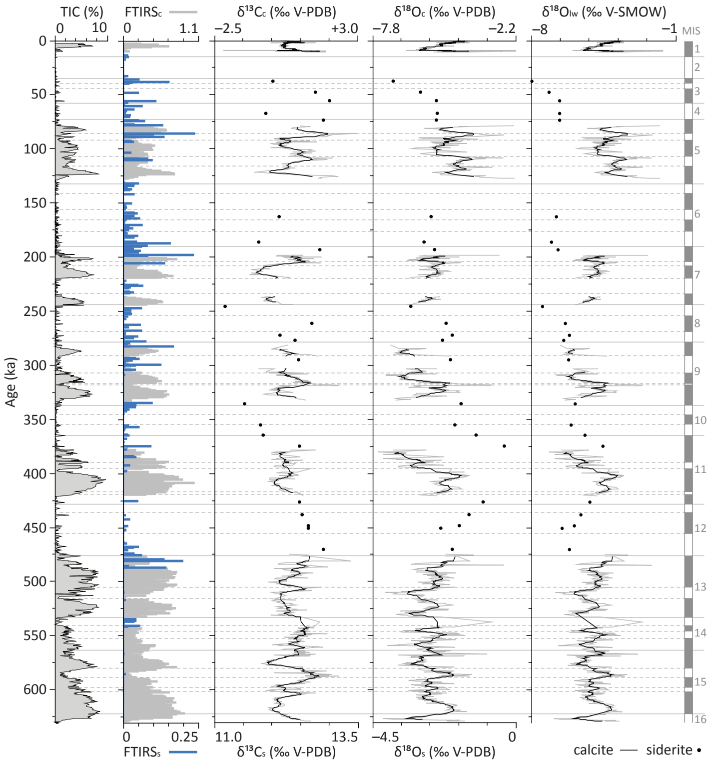

Figure 3. Isotope results from calcite ($\delta^{18}O_c$, $\delta^{13}C_c$), siderite ($\delta^{18}O_s$, $\delta^{13}C_s$), and calculated lakewater ($\delta^{18}O_{lw}$) from the Lake Ohrid SCOPSCO DEEP site composite profile, also showing TIC (Francke et al., 2015), the Holocene Co1262 calibration dataset ($\delta^{18}O_c$, $\delta^{13}C_c$; Lacey et al., 2014), and MIS stratigraphy (interglacial/interstadial = grey bar, glacial/stadial = white bar; Railsback et al., 2015). FTIRS results are shown for calcite (grey bars; calcite area = 707–719 cm^{-1}) and siderite (blue bars; siderite area = 854–867 cm^{-1}). Calcite data is given as raw (grey line) and 9-point running average (black line), siderite is presented as individual data points (black dots).

BGD
12, 13427–13481, 2015

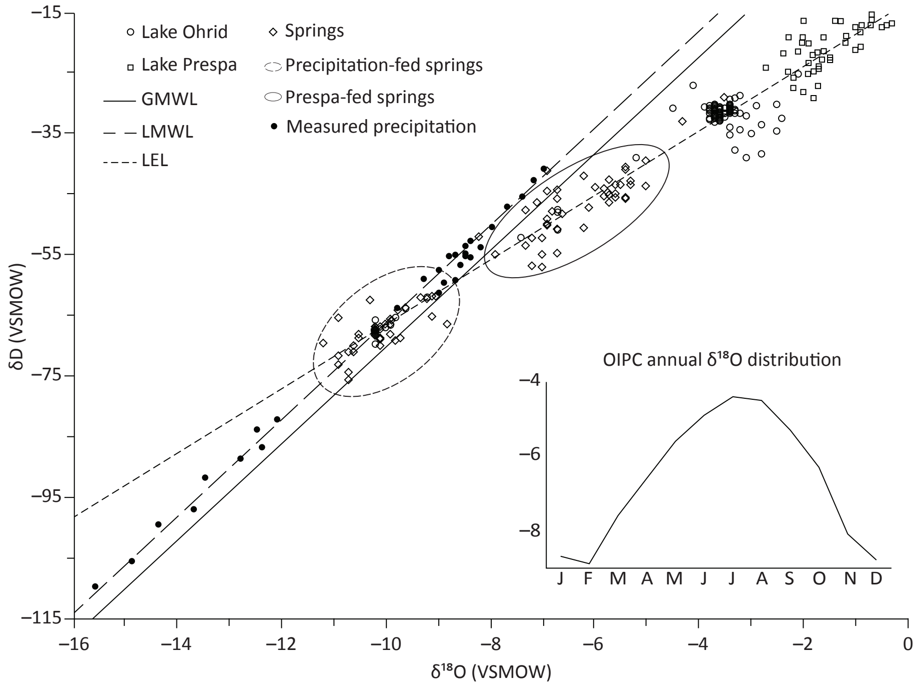

Figure 4. Modern isotope composition (δ^{18}O and δD) of waters from lakes Ohrid and Prespa, springs and local rainfall (Anovski et al., 1980, 1991; Eftimi and Zoto, 1997; Anovski et al., 2001; Matzinger et al., 2006a; Jordanoska et al., 2010; Leng et al., 2010a). The GMWL (Craig, 1961), LMWL (Anovski et al., 1991; Eftimi and Zoto, 1997) and calculated LEL are given. The annual distribution of δ^{18}O was calculated using the Online Isotopes in Precipitation Calculator (OIPC; Bowen et al., 2005; Bowen, 2015).

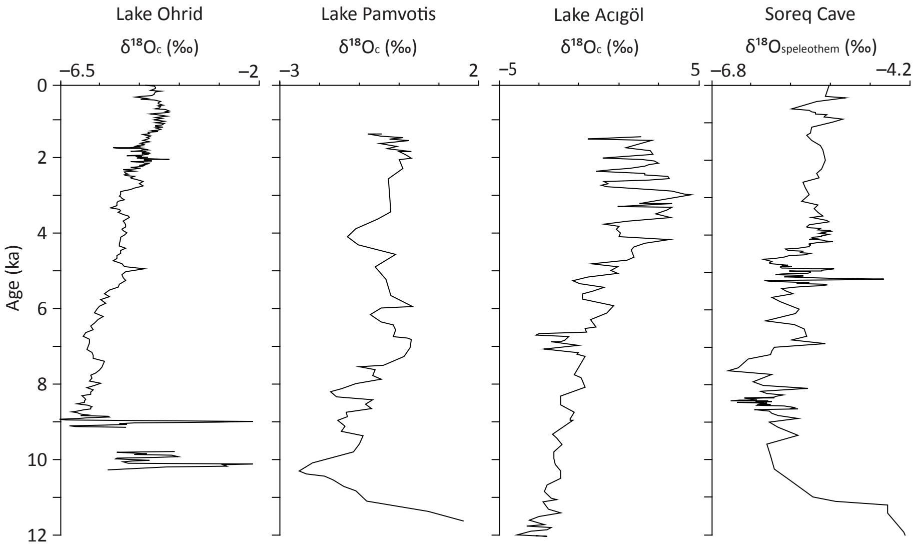

Figure 5. Comparison between the high resolution Holocene $\delta^{18}O_c$ calibration dataset from Lake Ohrid Lini core Co1262 (Lacey et al., 2014) and $\delta^{18}O$ from other regional records, including Lake Pamvotis, Greece (Frogley et al., 2001), Lake Acıgöl, Turkey (Roberts et al., 2001), and Soreq Cave, Israel (Bar-Matthews et al., 1999).

BGD
12, 13427–13481, 2015

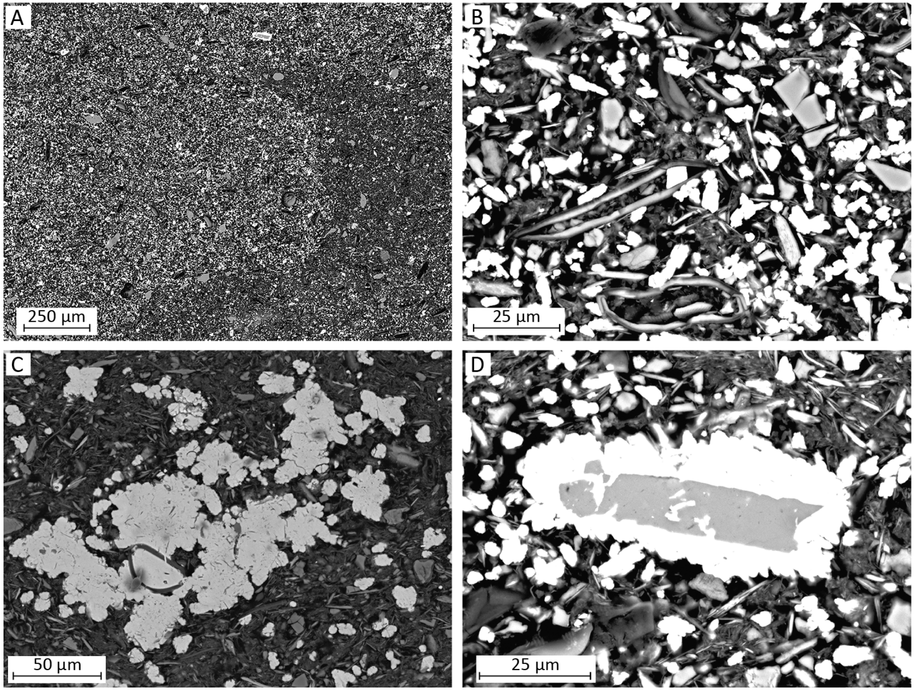

Figure 6. Backscatter SEM images of glacial sediment thin sections, showing **(a)** areas of high (brighter) and low (darker) siderite concentration in "burrow-like" structure, **(b)** area of high siderite concentration (white euhedral crystals) in an open-packed matrix (note: central diatom appears split by siderite crystal), **(c)** individual siderite crystals amalgamating to form a larger siderite crystal cluster, and **(d)** siderite overgrowth fringing a rare detrital dolomite grain.

BGD
12, 13427–13481, 2015

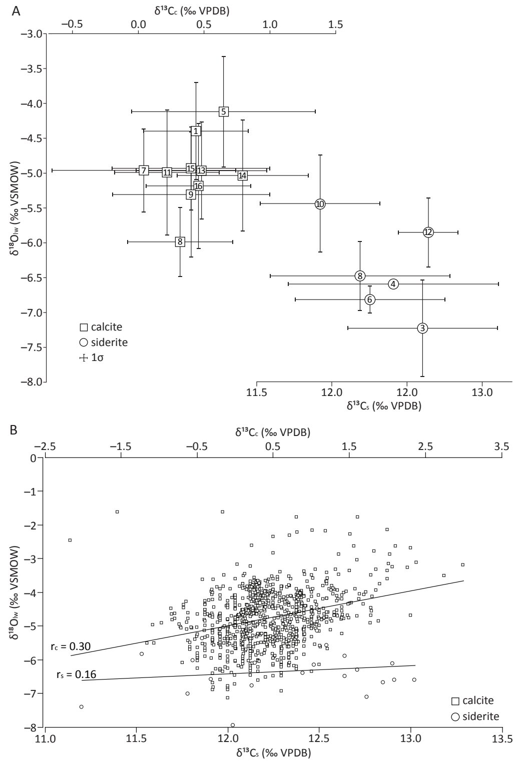

Figure 7. (a) $\delta^{18}O_{lw}$-$\delta^{13}C_c$ and $\delta^{18}O_{lw}$-$\delta^{13}C_s$ cross-plot showing the average and standard deviation (1σ) of each MIS (numbered center points) for both calcite and siderite data, **(b)** $\delta^{18}O_{lw}$-$\delta^{13}C_c$ and $\delta^{18}O_{lw}$-$\delta^{13}C_s$ cross-plot showing all calcite and siderite data and linear regression with Pearson correlation (r) (calcite r_c, $p = < 0.001$; siderite r_s, $p = > 0.1$). **(a)** and **(b)** both include the Lini site Holocene Co1262 calibration dataset (Lacey et al., 2014).

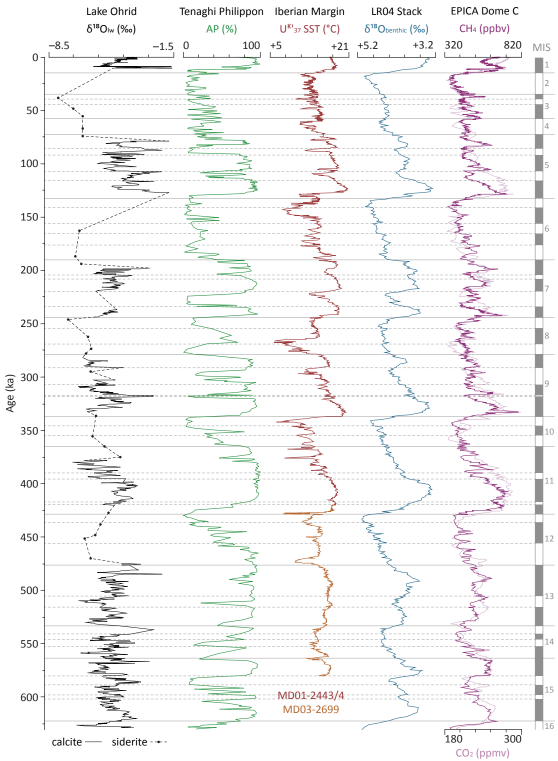

Figure 8. Comparison between Lake Ohrid $\delta^{18}O_{lw}$ and other climate records, including Tenaghi Philippon arboreal pollen (AP, Tzedakis et al., 2006), Iberian Margin $U^{K'}_{37}$-sea surface temperature composite profile (MD01-2443/4, 0–420 ka; Martrat et al., 2007; MD03-2699, 420–580 ka; Rodrigues et al., 2011), benthic $\delta^{18}O$ LR04 stack (Lisiecki and Raymo, 2005), Antarctic EPICA Dome C CH_4 and CO_2 (Loulergue et al., 2008; Lüthi et al., 2008), and MIS stratigraphy (interglacial/interstadial = grey bar, glacial/stadial = white bar; Railsback et al., 2015).

BGD
12, 13427–13481, 2015